CHAPTER 4

Visual Processing in the Primate Brain

CHRIS I. BAKER

VISUAL PROCESSING BASICS 81
THE RETINA 83
LATERAL GENICULATE NUCLEUS (LGN) 89
VISUAL AREAS IN PRIMATE CEREBRAL CORTEX 91
VISUAL TOPOGRAPHIC MAPS 92
V1—PRIMARY VISUAL CORTEX 93
V2 95
MAJOR CORTICAL VISUAL PROCESSING PATHWAYS 97
VENTRAL PATHWAY 97
DORSAL PATHWAY 101
LATERAL INTRAPARIETAL AREA (LIP) 103
CONCLUDING REMARKS 105
REFERENCES 105

Vision is the most widely studied and dominant sensory system in human and nonhuman primates. Of the total surface area of the cerebral cortex roughly 50% in macaque monkey, and 20 to 30% in human, is largely or exclusively involved in visual processing (Van Essen, 2004; Van Essen & Drury, 1997). Intensive study of vision in nonhuman primates, and particularly the macaque, has produced a detailed anatomical and functional description of processing at many levels of the neural visual pathway. In the past 20 years, the advent and development of functional brain imaging, and in particular functional Magnetic Resonance Imaging (fMRI), has enabled the detailed study of cortical, and in some cases subcortical, visual processing in humans. This chapter will synthesize findings from both human and nonhuman primates toward an understanding of the visual processing stream.

VISUAL PROCESSING BASICS

Vision is the process of extracting information about the external world from the light reflected or emitted by objects and surfaces. How light is reflected off an object or surface is determined by many factors including orientation, texture, movement, and absorbance. Thus, the reflected light carries information about those objects or surfaces and interpreting its pattern can aid an organism in interacting effectively with its environment. As an evolved biological system, the goal of vision is not to produce a veridical description of the external world but a description that facilitates adaptive behavior. Those aspects of the input that contain information critical for behavior will be emphasized and those aspects that carry little information will be discarded.

Vision begins at the eye with light passing through the cornea (refracts light), pupil (controls how much light enters the eye), and the lens (adjustably focuses light) onto the retina at the back of the eye. At the retina, photoreceptors convert the photons to electrochemical signals that are relayed along the optic nerve. The primary visual pathway from the optic nerves to the cerebral cortex passes through the dorsal Lateral Geniculate Nucleus (LGN) of the thalamus to the primary visual cortex (V1 or striate cortex) in the occipital lobes at the posterior of the brain.

In thinking about the challenges of visual processing, it is important to remember that primates receive visual input through two constantly moving eyes and process that information in two cerebral hemispheres. Each eye receives input from a limited area of visual space termed the *visual field* of that eye (Figure 4.1). Due to the horizontal separation of the eyes, their visual fields are spatially shifted and do not overlap completely. To produce a unified percept of the external environment, the brain must be able to align the images in the two eyes (Parker, 2007) and maintain and register information across eye movements (Melcher & Colby, 2008).

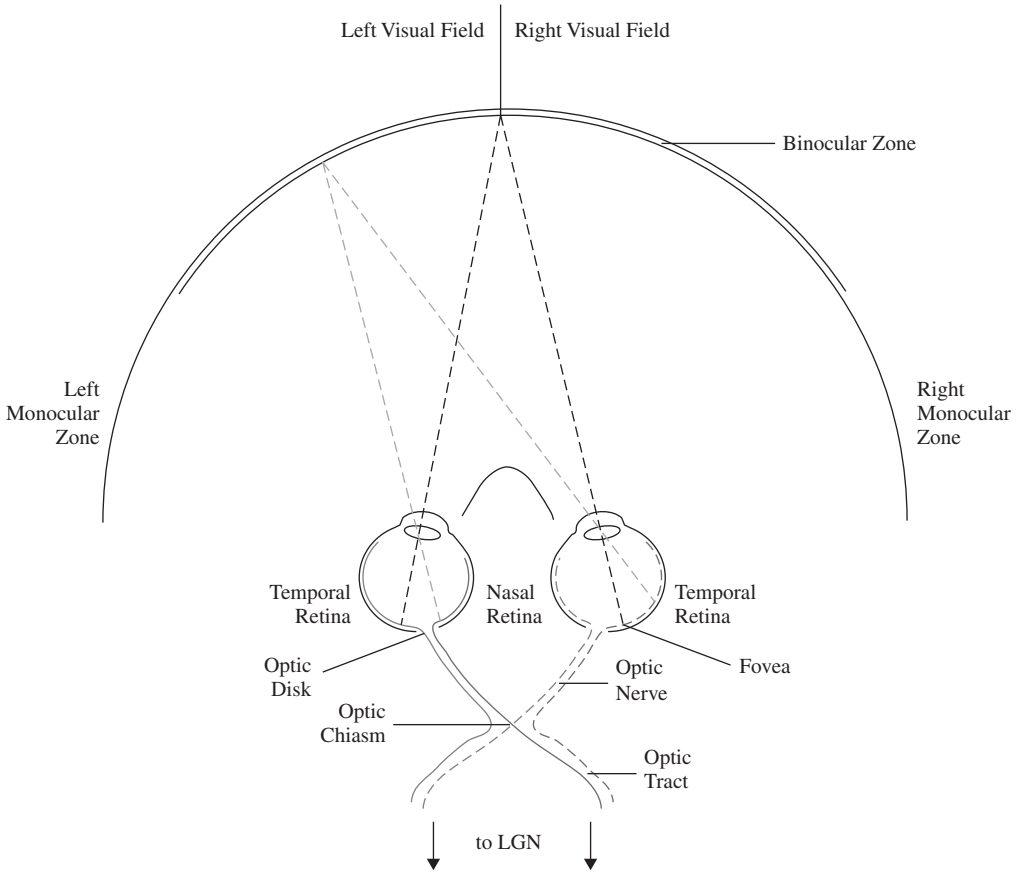

Figure 4.1 Visual fields and initial visual pathway. The overall visual field comprises a central binocular zone (double lines) and peripheral monocular zones (single lines). Size in vision is measured in terms of visual angle, the angle subtended on the retina. At a distance of 57 cm from the eyes, a stimulus 1 cm in size subtends 1 degree of visual angle. A useful approximation is that the width of the thumbnail at arms length is about 1.5 degrees of visual angle (O'Shea, 1991). The visual field of each eye is approximately 160 degrees and the overall visual field is approximately 200 degrees, with the binocular zone subtending approximately 120 degrees. Light from the point of fixation (thin dotted gray lines) falls on the fovea of each eye. In the binocular zone, light from the left visual field (thin black dotted lines) falls on the left nasal retina and the right temporal retina (and vice versa for light from the right visual field). The ganglion cell axons leave the retina via the optic disk. Signals from the left visual field are in dark gray, signals from the right visual field in light gray. Signals from the left eye are in solid lines, signals from the right eye in dotted lines. At the optic chiasm, the nerve fibers from the nasal retina of each eye crossover, so that each optic tract carries a complete representation of one half of the visual field to the contralateral LGN.

Within the binocular zone of the visual field, light reflected from the same point in space will hit the nasal retina in one eye and the temporal retina in the other eye (see Figure 4.1). These signals come together at the optic chiasm, where the optic nerves from the nasal retina of each eye crossover and join with the nerve fibers from the temporal retina of the other eye. Therefore, the optic tracts leaving the chiasm organize visual information by hemifield, with each tract conveying information about the contralateral visual field. This organization by visual field is maintained in the LGN and into V1. However, signals from the two eyes still remain segregated within each optic tract. Thus, each hemisphere receives visual input primarily from the contralateral visual field, segregated by eye, and later processing is required to produce a unified percept of visual space.

Parallel Processing in Vision

The visual signal arriving at the retina contains many different types of information including color, motion, and shape. Any extracted information may be used in many different ways and for many different behaviors. For example, reaching for your coffee mug requires precise information about the distance and orientation of the mug's handle, whereas recognizing your own mug likely depends on color, shape and size information. A general principle appears to be the evolution of specialized systems to

extract different types of commonly used visual information efficiently. In the primate visual system (Nassi & Callaway, 2009), and indeed many other sensory processing systems (K. O. Johnson & Hsiao, 1992; Kaas & Hackett, 2000), this leads to parallel processing in which independent, specialized cells and circuits extract specific types of information simultaneously from the same position in visual space. Such parallel processing is evidenced at multiple levels of visual processing, from the retina (Wassle, 2004) to high-level visual cortex (Ungerleider & Mishkin, 1982). For example, in the retina different populations of ganglion cells with different functional properties each tile the whole retina, providing multiple complete representations of the visual field and creating a series of parallel pathways to the next level of processing. Similarly, in the LGN, there are at least three different pathways (parvocellular, magnocellular, and koniocellular—see below) that appear to capture different aspects of the visual input such as motion and color. Finally, in the cortex, visual processing beyond V1 segregates into distinct dorsal and ventral pathways that primarily process spatial and nonspatial (visual quality) information, respectively. While parallel processing is efficient, it creates a challenge for later processing stages—integrating and consolidating the different streams of information to ultimately produce a unified and coherent percept.

This chapter focuses on what the structure, function, and connectivity at different levels of the visual processing pathway reveal about the types of computation being performed and highlights the divergence and convergence of multiple parallel processing pathways.

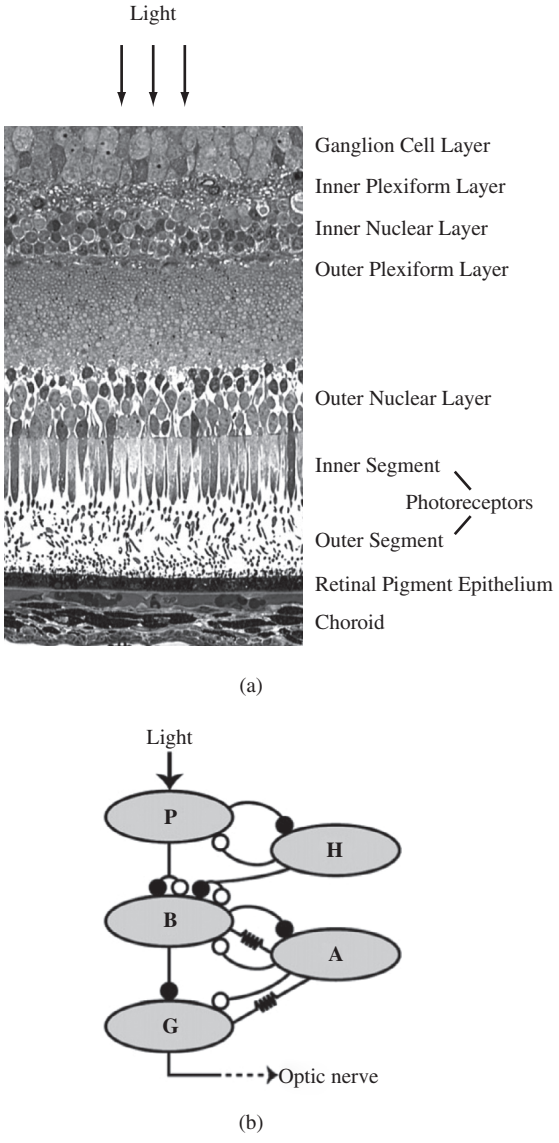

Figure 4.2 Structure of the retina. (a) Radial section through retina of Cynomolgus monkey (modified from Peters et al., 2007). Note that light has to pass through many different layers of the retina to reach the photoreceptors. At the fovea, the layers above the photoreceptors are displaced, forming a "foveal pit," allowing light to fall more directly on the densely packed cone photoreceptors in this region. (b) Schematic representation of the connections between different retinal cells. The solid and open circles represent excitatory and inhibitory chemical synapses, respectively. Resistor symbols indicate electrical coupling (gap junctions) between cells (from Gollisch & Meister, 2010). *Abbreviations:* B, bipolar cell; H, horizontal cell; A, amacrine cell; G, ganglion cell; P, photoreceptor.

THE RETINA

The retina is a sheet of neural tissue, 0.3–0.4 mm thick, that receives focused light from the lens of the eye. There are three primary dimensions defining light falling on the retina: position (two-dimensional location on the sheet), time, and wavelength (visible human range ~400–700 nm). Traditionally, the retina has been characterized as some sort of simple spatiotemporal filter prior to cortical processing, but recent results challenge this simplistic view (Gollisch & Meister, 2010).

There are at least 50 distinct types of retinal cell, grouped into five classes: photoreceptors, horizontal cells, bipolar cells, amacrine cells, and retinal ganglion cells (Masland, 2001a). These cells are arranged in a highly organized laminar structure (Figure 4.2). Although retinal cell types and structure are largely conserved across mammals (Wassle, 2004), the primate fovea, which enables high acuity vision, is unique (Gollisch & Meister, 2010). The following sections will briefly describe the properties of the different classes of retinal cell and the computations to which they contribute in the primate.

Photoreceptors

Specialization of visual processing begins with the photoreceptors of the retina. There are two different types, rods and cones, facilitating coverage of the full range of environmental light intensities. Rods are responsible for high-sensitivity, low-acuity vision (dim light: scotopic vision), responding to even single photons of visible light (Baylor, Lamb, & Yau, 1979). In the rod pathway, sensitivity is enhanced at the cost of spatial resolution by, for example, output from many individual rods converging onto a single rod bipolar cell (see below). In contrast, cones form the basis of color vision (Solomon & Lennie, 2007) and are evolutionarily older than rods (Okano, Kojima, Fukada, Shichida, & Yoshizawa, 1992). Relative to rods, cones have a much lower sensitivity, but higher acuity since there is much less spatial summation across individual cones, especially near the fovea (Curcio & Allen, 1990), and are responsible for daylight vision.

The spatial density of photoreceptors sets a fundamental limit on the spatial information available to higher levels of processing. The average human retina contains many more rods (∼90 million) than cones (∼4.5 million) but the distribution of the two photoreceptors

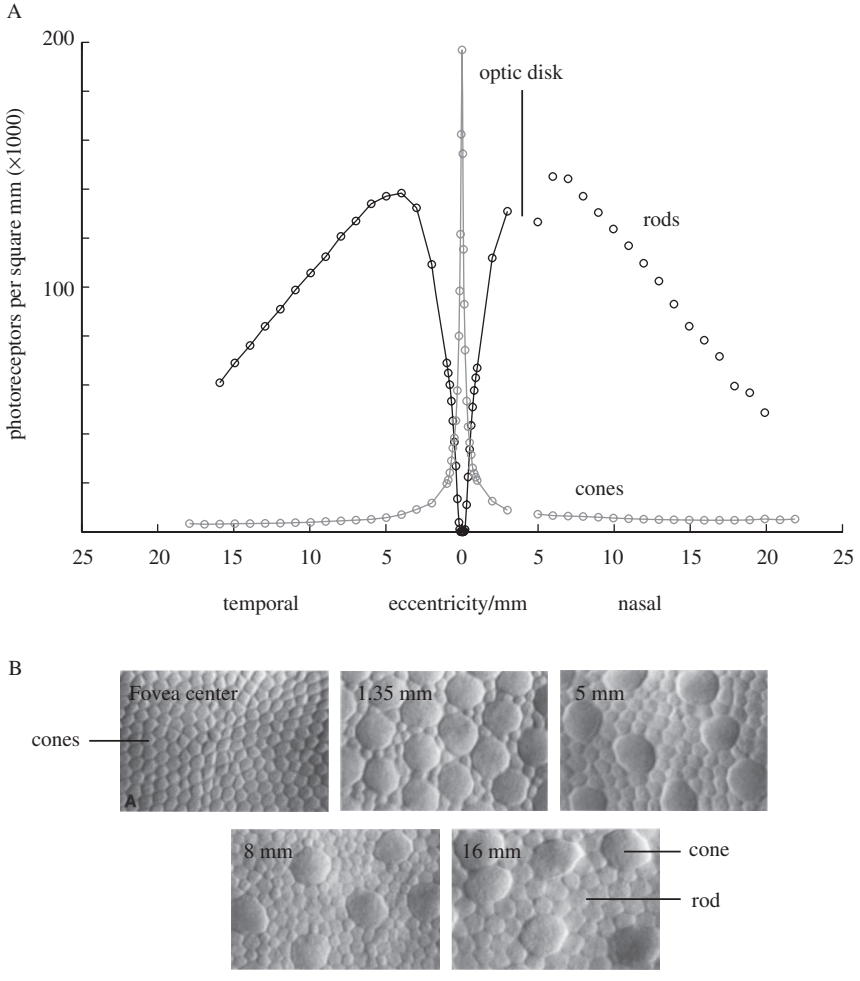

Figure 4.3 Photoreceptor distribution. (A) Density of rods (dotted line) and cones (solid line) across the horizontal meridian of the retina. Cones are predominantly located in the fovea with a peak density of ∼200,000 cones per mm^2 falling steeply with increasing eccentricity. Further, the distribution of cones is radially asymmetric around the fovea with greater density in nasal than temporal peripheral retina (Curcio, Sloan, Packer, Hendrickson, & Kalina, 1987; O. Packer et al., 1989). In contrast, the center of the fovea (∼0.35 mm diameter) is rod free with rod density increasing with eccentricity, peaking around the eccentricity of the optic disk. Interestingly, there is substantial between-individual variability in the distribution of photoreceptors (Curcio et al., 1987; O. Packer et al., 1989). (B) Optical sections of the cone mosaic from a single individual at different eccentricities in nasal retina. At the center of the fovea, there are only tightly packed cones present. With increasing eccentricity, the number of rods increases and the diameters of the cone inner segments also increase. Away from the center of the fovea, the larger profiles in the images are cones and the smaller profiles rods. Bar = 10 μm. (Replotted and modified from Curcio et al., 1990.)

differs significantly across the retina (Curcio, Sloan, Kalina, & Hendrickson, 1990). The peak density of cones is found in the fovea and falls off rapidly with eccentricity (Figure 4.3). In contrast, there is a rod free area within the fovea (~1.25 degrees diameter) with the density of rods increasing with eccentricity and peaking around the optic disk (where the optic nerve leaves the eye). In addition, for cones, but not rods, the inner segment, which serves as the light-catching aperture of the photoreceptor, increases with eccentricity (Packer, Hendrickson, & Curcio, 1989). Thus, while the maximum spatial resolution of the cone system decreases rapidly with eccentricity, its sensitivity increases.

While all photoreceptors respond to light throughout much of the visible spectrum, their peak sensitivity varies. Rods have peak sensitivity at a wavelength of ~500 nm. Further specialization occurs within cones, with different types of cone having different peak sensitivity. In some primates, including humans, there are three different types of cone (Baylor, Nunn, & Schnapf, 1987) giving rise to "trichromatic" vision. These cones have peak sensitivity to short (S, ~430 nm), medium (M, ~530 nm) or long (L, ~560 nm) wavelengths (Figure 4.4). S cones constitute only 5% of all cones, form a semiregular array, are absent from the center of the fovea, and have peak density at 1 degree (DeMonasterio, Schein, & McCrane, 1981; Martin & Grunert, 1999). However, there is a highly variable ratio and somewhat random distribution of L to M cones that differs across the retina (Deeb, Diller, Williams, & Dacey, 2000; Hofer, Carroll, Neitz, Neitz, & Williams, 2005).

Analysis of color requires the comparison of signals from different types of cones and consistent with psychophysical observations, there are red-green (L versus M) and blue-yellow (S versus L + M) opponent signals in the cone pathways.

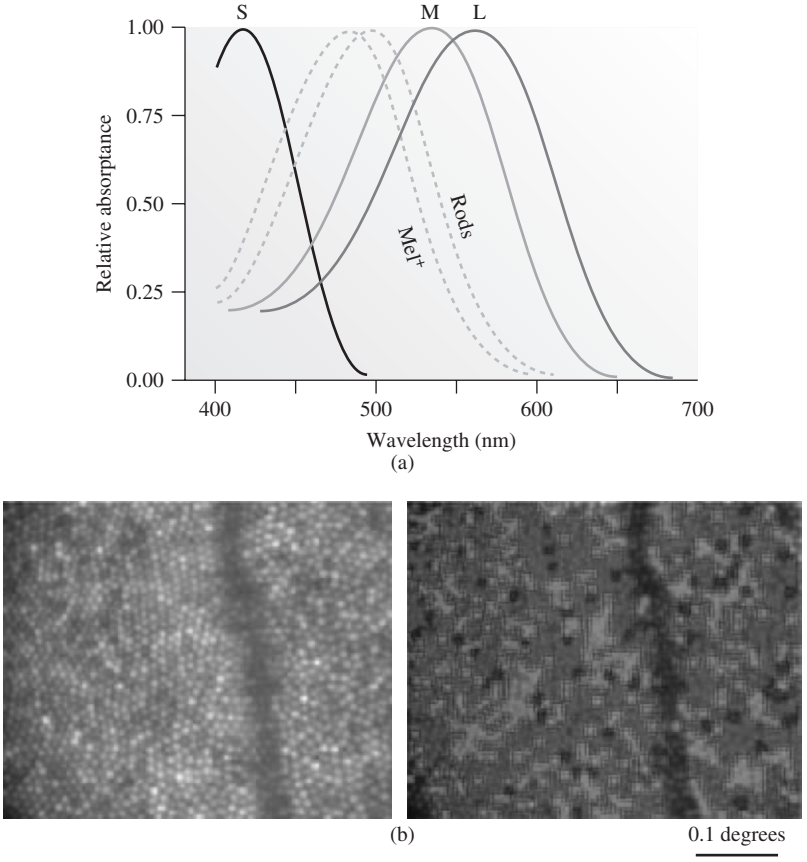

Figure 4.4 Sensitivity and distribution of cone photoreceptors. (Color image on page C1.) (a) S- (blue-line), M- (green-line), and L- (red-line) cones respond to light throughout much of the visible spectrum but show different peak sensitivity. For comparison the dotted lines show rods and the recently discovered photosensitive ganglion cell. (b) Spatial distribution of photorecpetors in the human retina, 0.8 degrees from fovea. The left panel shows the arrangement of photoreceptors. The right panel shows the cones (S, M, L) colored according to spectral sensitivity. The S-cones are relatively sparse but form a semiregular array. The L- and M-cones are distributed randomly with frequent clumping. (Modified from Solomon & Lennie, 2007.)

Horizontal Cells

There are two main types of horizontal cell in mammals (Wassle & Boycott, 1991), providing feedback to photoreceptors and bipolar cells. H1 cells contact both rods and cones, whereas H2 cells contact cones only (Masland, 2001b; Wassle et al., 2000). Since horizontal cells pool light from a larger area than photoreceptors, they effectively produce center-surround antagonism by subtracting a broad response from a local signal (Verweij, Hornstein, & Schnapf, 2003; Wassle, 2004), ideal for detecting local changes in input. Importantly, horizontal cell feedback creates the first stage of red-green (Crook, Manookin, Packer, & Dacey, 2011) and blue-yellow (O. S. Packer, Verweij, Li, Schnapf, & Dacey, 2010) opponency in the retina.

Bipolar Cells

There are 11 types of bipolar cell in primates (Boycott & Wassle, 1991; Chan, Martin, Clunas, & Grunert, 2001; Joo, Peterson, Haun, & Dacey, 2011), 10 linked to cones and only 1 to rods. Rod bipolar cells contact between 6 (at fovea) and 40 (in periphery) rods (Wassle, 2004) and connect to ganglion cells only indirectly via amacrine cells that synapse onto cone bipolar terminals. This type of organization may reflect the late evolution of rods (Masland, 2001a).

Each cone connects to several different types of bipolar cell. Thus, even at this first synapse in the retina, the cone signals diverge into multiple parallel pathways. Cone bipolar cells are stratified within the inner plexiform layer of the retina confining their synapses to cells at the same level and segregating their connections with different types of retinal ganglion cell. The output of cones is separated into ON and OFF types, excited by light onset or offset, respectively. Cone bipolar cells fall into two main categories with distinct morphology: midget and diffuse. While diffuse bipolar cells contact between 5 and 10 cones, midget bipolar cells can exclusively connect with single cones and synapse on to a dedicated class of midget retinal ganglion cells (Masland, 2001b), enabling the greatest possible spatial resolution.

Amacrine Cells

There are at least 30 distinct types of amacrine cells in mammals (MacNeil, Heussy, Dacheux, Raviola, & Masland, 1999). Amacrine cells are inhibitory interneurons that connect with bipolar cells, ganglion cells, and other amacrine cells, providing the major synaptic input to ganglion cells (Jacoby, Stafford, Kouyama, & Marshak, 1996). Although the different types of amacrine cells have different connections and neurotransmitters, suggesting distinct functions, their precise roles are poorly understood, except in a few cases. For example, AI amacrine cells have wide-spreading axonlike processes that cover long retinal distances (Stafford & Dacey, 1997) and are likely involved in computations enabling detection of object motion (Olveczky, Baccus, & Meister, 2003). Similarly, starburst amacrine cells (so called because of their radiating dendrites), found in many mammalian species, provide a feedforward excitation onto ganglion cells that is selective for motion-direction (Euler, Detwiler, & Denk, 2002; Hausselt, Euler, Detwiler, & Denk, 2007).

Ganglion Cells

At least 17 distinct ganglion cell types have been identified, distinguished by the size and branching patterns of their dendritic trees, of which at least 13 project to the LGN (Dacey, 2004; Dacey, Peterson, Robinson, & Gamlin, 2003). The responses of a ganglion cell are often described in terms of its receptive field, the region of visual space over which stimuli elicit a response. Although often represented as Gaussians, ganglion cell receptive fields are irregular in shape but interlock to tightly map visual space (Gauthier, Field, Sher, Greschner et al., 2009). Further, the receptive fields of each ganglion cell type tile the whole retina (Field & Chichilnisky, 2007; Field et al., 2007), so a single spot of light at one point of the retina can stimulate multiple ganglion cell types conveying information in parallel to the brain (Wassle, 2004) (Figure 4.5). While differences in morphology may indicate functional differences this is not necessarily the case. For example, some ganglion cells show nearly identical receptive field overlap despite differences in dendritic overlap and this may reflect compensation within the circuitry for morphological differences (Gauthier, Field, Sher, Shlens et al., 2009).

Ganglion cell receptive fields typically have a central region with a concentric surround and may be ON center/OFF surround or OFF center/ON surround (Kuffler, 1953). The dendrites of ON center and OFF center ganglion cells stratify in either the inner or outer part of the inner plexiform layer, respectively, with their center response driven by corresponding ON or OFF bipolar cells. Additionally, differences in stratification within each part of the inner plexiform layer further separate different types of ganglion cells (Dacey, 2004) (Figure 4.6).

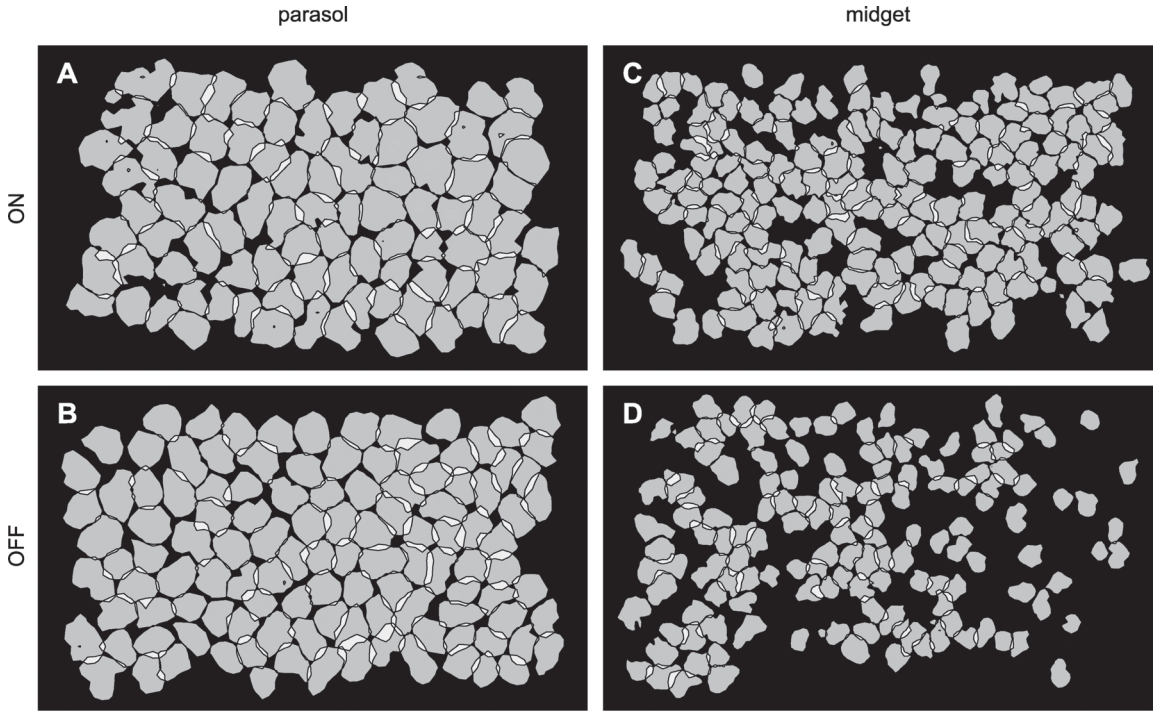

Figure 4.5 Retinal ganglion cell receptive fields are irregularly shaped, tightly interlock, and tile the whole retina. Contour lines representing simultaneously recorded receptive fields from four different types of ganglion cell in macaque retina. (A) ON parasol cells. (B) OFF parasol cells. (C) ON midget cells. (D) OFF midget cells. Gaps in the mosaic reflect undersampling of cells rather than gaps in the retinal representation. (Modified from Gauthier, Field, Sher, Greschner et al., 2009.)

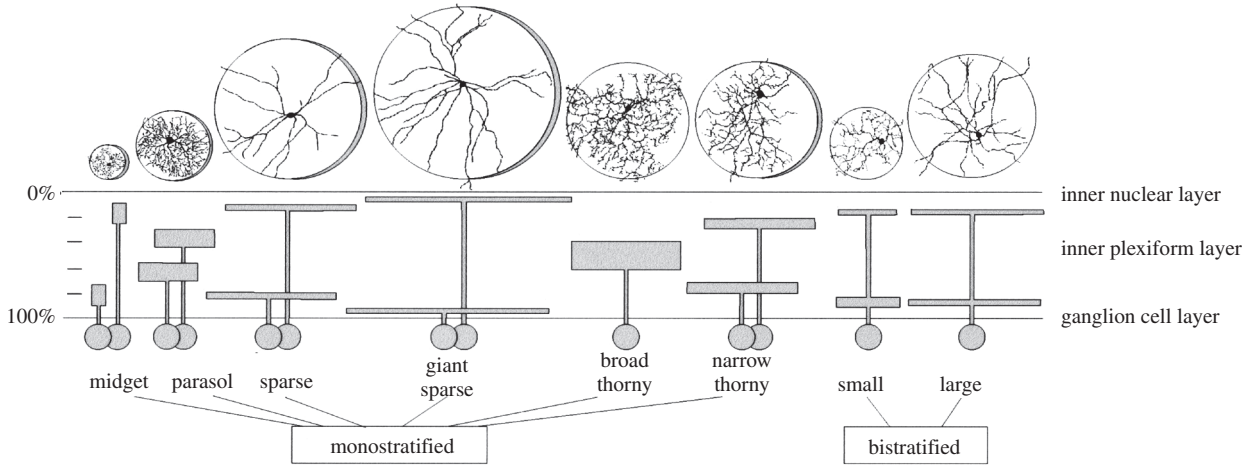

Figure 4.6 Types of retinal ganglion cell. Schematic representations of 13 different types of monostratified and bistratified ganglion cells. The width of the horizontal bars indicates the extent of the dendritic arbors and the vertical height of the bars indicates their location within the inner plexiform layer. (Modified from Dacey, Peterson, Robinson, & Gamlin, 2003.)

Only three types of retinal ganglion cell have been thoroughly characterized: midget, parasol, and bistratified. Midget and parasol cells together comprise over 65% of ganglion cells, and the bistratified cells around 35% (Dacey, 2004). These different types of ganglion cell are thought to be the origin of the parvocellular, magnocellular, and koniocellular pathways, respectively, that are anatomically segregated through the LGN and into V1. For this reason, the midget ganglion cells are often referred to as P-cells and the parasol ganglion cells as M-cells.

Midget Cells

The primary functional role of midget ganglion cells has been the subject of some controversy (Dacey, 2004). On the one hand, the midget ganglion cells appear well-suited to support high acuity vision with small receptive fields (Calkins & Sterling, 1999). Close to the fovea, each midget ganglion cell receives its input from a single midget bipolar cell, which in turn connects to a single cone. At the peak of the cone distribution, there are two midget ganglion cells for every cone (Ahmad, Klug, Herr, Sterling, & Schein, 2003). On the other hand, by reflecting the input to a single cone, the midget ganglion cells might be critical for comparison of signals from different cones and thus for color vision (Reid & Shapley, 2002). Consistent with this hypothesis, they do exhibit opponency of L- and M-cone signals, with stimulation of one type of cone causing excitation and the other inhibition. Alternatively, it might be that midget cells play a critical role in both high acuity and color vision.

In peripheral retina, where ganglion cells pool signals from many cones, the nature and purity of the L- and M- cone inputs to the center and surround of midget cell receptive fields has been the subject of much debate. For example, L-M opponency could be produced by (a) pure L- or M-cone center signals with random sampling in the surround (e.g., Martin, Lee, White, Solomon, & Ruttiger, 2001), or (b) relatively pure signals in both center and surround (e.g., Buzas, Blessing, Szmajda, & Martin, 2006). Alternatively, it has been suggested that there is random cone sampling (Diller et al., 2004). Simultaneous recording of hundreds of retinal ganglion cells and subsequent mapping of all the cone inputs revealed dominant or exclusive L- or M-cone input in the receptive field center of midget cells with strong opponency (Field et al., 2010), demonstrating selective sampling that is not merely a reflection of the local density of L- and M-cones (Figure 4.7).

Parasol Cells

Compared to midget cells, parasol cells have much larger receptive fields, higher contrast, and higher temporal frequency sensitivity, suggesting a role in motion processing. They receive input from multiple cone bipolar cells, and are stratified near the middle of the inner plexiform layer (Dacey, 2004). Parasol cells pool across both L- and M-cones and, hence, respond strongly to achromatic stimuli.

Small Bistratified Cells

Small bistratified ganglion cells have receptive fields similar in size to parasol cells. They exhibit a strong ON response from the S cones, conveyed by selective blue cone bipolar cells, with an inhibitory input from L- and M-cones (Field et al., 2007). S-cone input is also observed in OFF midget cells, but very rarely in ON midget cells or any parasol cells (Field et al., 2010).

Other Ganglion Cells

Other types of ganglion cells that have been identified include large bistratified cells (another S-ON chromatic pathway), sparse monostratified cells (an S-OFF chromatic pathway), and smooth monostratified cells (Dacey, 2004). Many of these other types of ganglion cell are only found in small numbers. Importantly, however, this may simply be a reflection of the spatial sampling density (many have large dendritic fields) and not be indicative of overall significance in visual processing (Field & Chichilnisky, 2007). Indeed, the less common ganglion cell types in primates collectively provide more capacity than the entire cat retina (Wassle, 2004).

Two recently discovered types of retinal ganglion cell are of particular interest. First, there are photosensitive ganglion cells that express melanopsin (Berson, 2003; Dacey et al., 2005). These cells exhibit a much slower light response than rods or cones and are important for control of circadian rhythms and the pupillary light reflex (Gooley, Lu, Fischer, & Saper, 2003). Second, upsilon ganglion cells (identified based on functional rather than morphological properties) have large receptive fields and exhibit highly nonlinear spatial summation (Petrusca et al., 2007). These cells may be the equivalent of the Y-cells reported in other mammalian species that are thought to signal texture motion with no directional selectivity (Gollisch & Meister, 2010).

Optic Nerve

The axons from all retinal ganglion cells stream towards the optic disk in the nasal retina of each eye and form the optic nerve. There are no photoreceptors at the optic disk, producing a "blind spot" in the visual field of each eye. However, the blind spot for each eye receives some

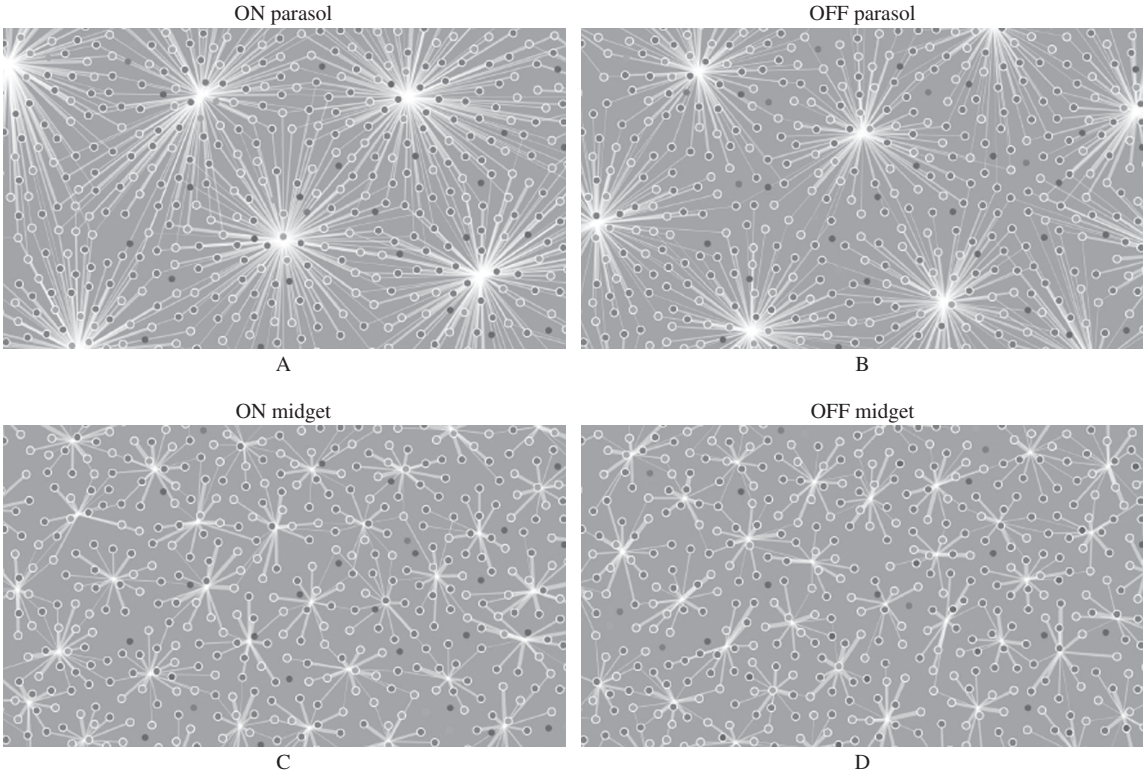

Figure 4.7 Functional connectivity in the retina. (Color image on page C1.) Simultaneous recording of hundreds of retinal ganglion cells and identification of the photoreceptors contributing to the receptive field center of each cell produces a detailed picture of the connectivity in the retina. Each panel shows a different type of ganglion cell (ON and OFF midget and parasol cells). Red, green, and blue circles are the L-, M-, and S-cones. Cones giving input to at least one ganglion cell are circled in white. White lines indicate cones contributing to the receptive field center with the thickness of each line proportional to weight. Note that S-cones largely contribute only to OFF midget cells. Scale bar = 50 μm. (From Field et al., 2010.)

input from the other eye and we are not normally aware of them.

There are at least 15 distinct targets in the brainstem for projections in the optic nerve (Kaas & Huerta, 1988; Rodieck & Watanabe, 1993). The vast majority of ganglion cells (~90%) project to the LGN (Perry, Oehler, & Cowey, 1984). There are six other major targets including the superior colliculus (involved in the control of eye movements), suprachiasmatic nucleus (involved in the regulation of circadian rhythms), the inferior pulvinar (high-order relay conveying signals between cortical areas), and the pretectum (involved in adjusting pupil size).

In summary, the retina receives light input, which is converted to electrochemical signals and passed through highly specific and parallel circuits culminating in responses in at least 17 distinct ganglion cell populations that project out of the retina. Rather than being a simple spatiotemporal filter, the circuits in the retina are capable of computations for extracting information such as texture motion and motion-direction. The following section will follow these signals to the LGN, which provides the major input to the cerebral cortex.

LATERAL GENICULATE NUCLEUS (LGN)

Located in the posterior part of the thalamus, the LGN is often viewed as a simple relay as signals pass from retina to cortex. However, the LGN also receives extensive input from nonretinal sources (including brainstem and feedback from cortex), that in combination exceed the retinal input, and it appears to be actively involved in the regulation of visual input to cortex (Briggs & Usrey, 2011; Casagrande, Sary, Royal, & Ruiz, 2005; Sherman & Guillery, 2002). Despite the small size of the LGN and the limited spatial resolution of fMRI, recent studies have started to reveal its functional organization in humans (Kastner, Schneider, & Wunderlich, 2006).

The LGN is largely a six-layered structure, reduced to four layers in regions responding to eccentric locations in the visual field beyond the optic disk (Kaas, Guillery, & Allman, 1972; Malpeli & Baker, 1975) (Figure 4.8). Each layer receives input from one eye, with layers 1, 3, and 5 (numbered from ventral to dorsal) receiving input from nasal retina of the contralteral eye, and layers 2, 4, and 6 receiving input from temporal retina of the ipsilateral

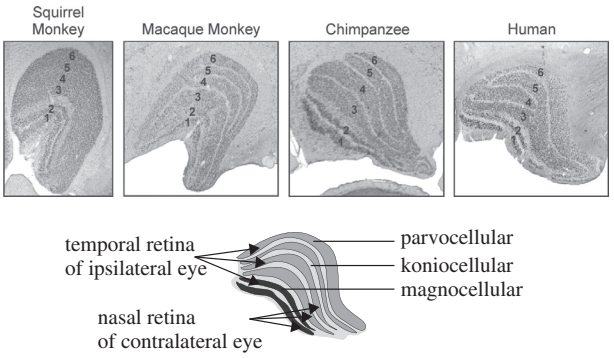

Figure 4.8 Organization of LGN. Top row shows the LGN in four different species of primate. In all species, the LGN has six layers with the magnocellular, parvocellular, and koniocellular neurons occupying distinct layers. Bottom row shows a schematic of the organization of the LGN and its inputs. (Modified from Briggs & Usrey, 2011.)

eye. In human and macaque, layers 1 and 2 contain magnocellular neurons, which receive input primarily from the parasol ganglion cells, while layers 3-6 contain parvocellular neurons, which receive input primarily from the midget ganglion cells. Intercalated between these six layers are koniocellular neurons (Hendry & Reid, 2000; Hendry & Yoshioka, 1994), which receive input primarily from the bistratified ganglion cells. Each koniocellular layer is innervated by the same retina that innervates the immediately overlying M or P layer (Hendry & Reid, 2000). Parvocellular neurons are the most numerous in the LGN, but there are roughly equal numbers of magno- and koniocellular neurons (Blasco, Avendano, & Cavada, 1999). Given this layered structure, the standard model of visual processing in the primate has been of three LGN-defined "pathways" from retina to cortex (magnocellular, parvocellular, and koniocellular). However, this is likely to be an oversimplification. First, the magnocellular layers are composed of more than one cell type, possibly reflecting input from nonparasol as well as parasol cells (Kaplan & Shapley, 1982). Second, there are multiple types of cells in koniocellular layers with different spatial, temporal, and contrast characteristics, likely reflecting inputs from multiple types of ganglion cells (Hendry & Reid, 2000; Xu et al., 2001).

In addition to the organization by eye, the LGN is also retinotopically organized, with an ordered map of contralateral visual space in each layer. In macaques, the representation of the horizontal meridian divides the LGN into a superior and medial half corresponding to the lower visual field and an inferior and lateral half corresponding to the upper visual field. Eccentricity is represented serially along the posterior-anterior dimension with the fovea represented at the posterior pole. A similar organization is found in the human LGN (W. Chen, Zhu, Thulborn, & Ugurbil, 1999; Schneider, Richter, & Kastner, 2004).

The receptive fields of LGN neurons are very similar to those observed in retinal ganglion cells showing center-surround antagonism (ON center, OFF surround and vice versa) and increasing in size with retinal eccentricity (Xu, Bonds, & Casagrande, 2002; Xu et al., 2001). In addition, LGN neurons exhibit modulation by stimuli that extend beyond the classical receptive field, often referred to as the suppressive surround since any stimuli (on or off) reduce the neuronal response (Solomon, White, & Martin, 2002). Surround suppression is stronger for magnocellular than parvocellular and koniocellular neurons (Solomon et al., 2002) and is produced by feedforward mechanisms from the retina, rather than feedback from the cortex (Alitto & Usrey, 2008). This type of suppressive effect controls the gain of LGN neurons.

The functional properties of magnocellular and parvocellular neurons are also similar to those observed for parasol and midget ganglion cells, respectively (e.g., Alitto, Moore, Rathbun, & Usrey, 2011; Derrington & Lennie, 1984; Kaplan & Shapley, 1982, 1986). Magnocellular neurons respond better to low contrast stimuli and have sensitivity to higher temporal frequencies than parvocellular neurons. Most parvocellular neurons have color-opponent (red-green) center-surround receptive fields and at any given eccentricity have higher spatial resolution than magnocellular neurons (Shapley, Kaplan, & Soodak, 1981). The functional properties of koniocellular neurons have been less well studied (in part due to the difficulty of isolating these neurons, especially in macaque) and are very diverse (e.g., Irvin, Norton, Sesma, & Casagrande, 1986; White, Solomon, & Martin, 2001). However the majority of cells carrying S-cone signals are located in the koniocellular layers (Roy et al., 2009). This means that in the LGN there is an anatomical separation between neurons carrying red-green (parvocellular layers) and those carrying blue-yellow (koniocellular layers) opponent signals.

Nonretinal Inputs to LGN

The LGN receives only 30–40% of its input from the retina (Wilson & Forestner, 1995). Neurons originating in the cortex comprise the largest source of synaptic input (Erisir, Van Horn, Bickford, & Sherman, 1997; Erisir, Van Horn, & Sherman, 1997). In addition, there are inputs from the visual sector of the thalamic reticular nucleus, the superior colliculus (primarily to the koniocellular layers) and

other brainstem structures (Casagrande et al., 2005). The feedback from V1 appears to maintain three separate pathways with three groups of corticogeniculate neurons whose properties resemble those of the neurons in the parvocellular, magnocellular, and koniocellular layers (Briggs & Usrey, 2009) with projections into distinct layers in the LGN (Fitzpatrick, Usrey, Schofield, & Einstein, 1994; Ichida & Casagrande, 2002). Thus, feedback from the cortex can provide a stream-specific modulation of LGN processing. This feedback from the cortex multiplicatively increases the response of both magnocellular and parvocellular LGN neurons (Przybyszewski, Gaska, Foote, & Pollen, 2000) and attention can modulate responses in LGN in both monkey (McAlonan, Cavanaugh, & Wurtz, 2008) and human (O'Connor, Fukui, Pinsk, & Kastner, 2002). Further, activity in human LGN correlates strongly with the perceived stimulus in binocular rivalry, an experimental paradigm in which stimuli presented separately to each eye compete for representation and subjects perceive only one stimulus at a time (Wunderlich, Schneider, & Kastner, 2005). These properties are consistent with a role for the LGN beyond a simple relay, and suggest involvement in controlling attentional response gain and visual awareness (Kastner et al., 2006).

In summary, the LGN receives input from the different retinal ganglion cell populations in the retina as well as descending inputs from V1. The major output of the LGN is to layer 4 of primary visual cortex (V1), and the LGN may be involved in actively controlling the input to cortex rather then simply relaying information. The following sections will briefly discuss the overall organization of visual areas in the cortex before discussing V1 in detail.

VISUAL AREAS IN PRIMATE CEREBRAL CORTEX

The cerebral cortex is typically parcellated into a number of distinct areas based on measured differences in (a) architechtonics (e.g., differences in laminar structure), (b) connectivity, (c) visual topography (maps of visual space), and (d) functional properties (Felleman & Van Essen, 1991). However, different studies have emphasized different combinations of these criteria and many different parcellation schemes have been proposed (Van Essen, 2004). Consensus has only been achieved for a limited number of areas, including V1, V2, V4, and the middle temporal area (MT). Further, for many areas it is hard to identify the homologues in different primate species (Rosa & Tweedale, 2005). Overall, there is evidence for at least 40 anatomically and/or functionally distinct subdivisions of visually responsive cortex in the macaque (Van Essen, 2004).

In general, there are three different types of long-range connection within and between these cortical areas supporting visual processing: feedforward, feedback, and horizontal (or intrinsic) connections (for detailed review, see Bullier, 2004). Feedforward connections transfer information away from the thalamic input (e.g., LGN → V1 → V2) (Shipp, 2007). In contrast, feedback connections link cortical areas in the opposite direction. Finally, horizontal connections link neurons within a cortical area and facilitate the local processing of information in conjunction with short-range vertical connections between cortical layers.

Most of cortex, including sensory cortex, comprises six layers and the different types of connections within and between cortical areas are often layer-specific (Figure 4.9). Feedforward connections, including those from the LGN, project to layer 4 (Rockland & Pandya, 1979), which contains many small densely packed cells and is often referred to as the "granular layer." These connections typically originate in layers 2/3 of lower cortical areas. In contrast, feedback connections often originate in the infragranular layers (5/6) and typically project to layers 1 and 5/6 of the lower area. Finally, horizontal connections are reciprocal intralaminar projections (Rockland & Lund, 1983) and exhibit patchy termination patterns that may correspond with underlying functional properties (Malach, Amir, Harel, & Grinvald, 1993; Yoshioka, Blasdel, Levitt, & Lund, 1996).

Thus, the cortex contains many visual areas with elaborate connectivity within and between them facilitating the processing of visual information. The next section focuses on one property often used to define a visual area, the presence of discrete visual topography.

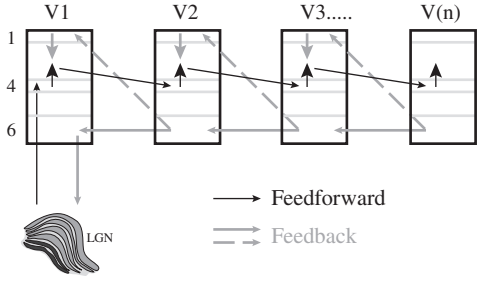

Figure 4.9 Laminar characteristics of connections between cortical areas. Schematic characterization of the main pathways for feedforward and feedback processing within visual cortex. (Adapted from Shipp, 2007.)

VISUAL TOPOGRAPHIC MAPS

A common feature of visual cortex is retinotopic organization, similar to that observed in LGN. For example in V1, neighboring neurons respond to stimuli presented at adjacent locations in the visual field and the arrangement of responses constitutes an ordered map of visual space. There are a multitude of such retinotopic maps throughout visual cortex, and the presence of a complete map of visual space is one of the criteria used to define a distinct cortical area. While these maps were first identified based on human patients with lesions to visual cortex (Horton & Hoyt, 1991) and invasive studies in nonhuman primates (e.g., Hubel & Wiesel, 1974; Tootell, Silverman, Switkes, & De Valois, 1982), the advent of fMRI has enabled the simultaneous and noninvasive elucidation of multiple visual field maps in both human (Arcaro, McMains, Singer, & Kastner, 2009; Wandell, Dumoulin, & Brewer, 2007) and monkey (Arcaro, Pinsk, Li, & Kastner, 2011; Brewer, Press, Logothetis, & Wandell, 2002). While there are many similarities between human and monkey, more field maps have been identified in human and there may be differences in the mapping even in areas as early as V4 (Winawer, Horiguchi, Sayres, Amano, & Wandell, 2010).

Visual field maps can be identified with fMRI by systematically varying the location of a stimulus in the visual field (Figure 4.10). They are defined with respect to a fixation point, and thus, the fovea. There are two principal dimensions to retinotopic maps: distance from the fovea (eccentricity) and angular distance from the horizontal and vertical meridians (polar angle). Commonly, the maps can be measured by varying either the eccentricity of a ring stimulus or the polar angle of a wedge stimulus in the visual field and identifying the optimal eccentricity and angle of a stimulus from fovea for each location in the cortex (DeYoe et al., 1996; Engel et al., 1994; M. I. Sereno et al., 1995).

Using these methods, field maps have been identified in the occipital lobe (corresponding to V1, V2, and V3) (Brewer et al., 2002; Dougherty et al., 2003; M. I. Sereno et al., 1995), in dorsal regions extending into parietal cortex (Arcaro et al., 2011; Swisher, Halko, Merabet, McMains, & Somers, 2007) and in lateral and ventral regions extending into the temporal lobe (Arcaro et al., 2009; Brewer, Liu, Wade, & Wandell, 2005; Larsson & Heeger, 2006). Further, systematic manipulations of the location of attention or eye movements in visual space have also identified maps in parietal cortex (Schluppeck, Glimcher, & Heeger, 2005; M. I. Sereno, Pitzalis, & Martinez, 2001; Silver, Ress, & Heeger, 2005).

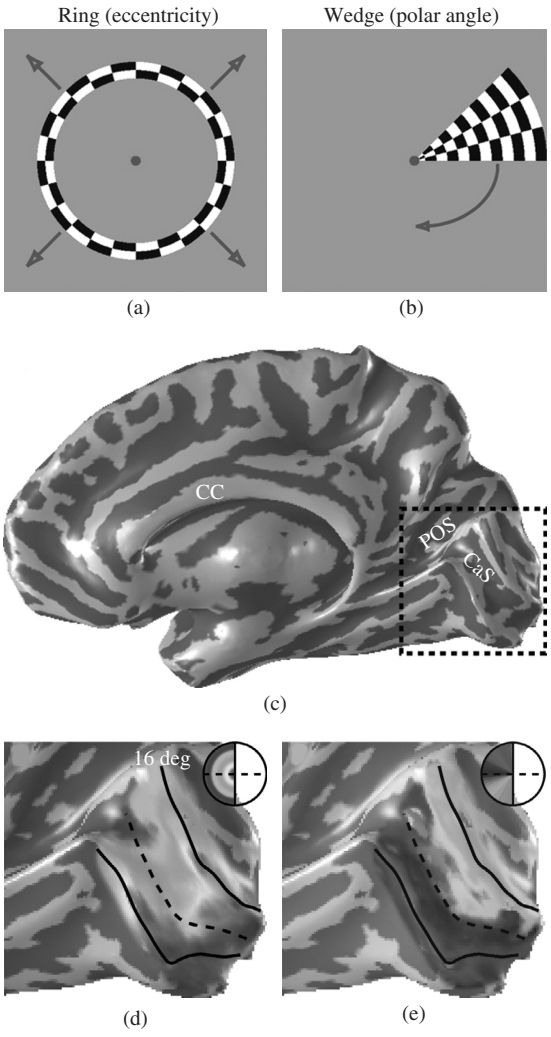

Figure 4.10 Identifying visual field maps. (Color image on page C2.) Retinotopy can be measured by varying the eccentricity of a ring stimulus (a) and the angle of a wedge stimulus (b) and determining the optimal eccentricity and angle for every voxel in the brain (c). The expanded view of the medial occipital cortex shows the maps obtained for eccentricity (d) and polar angle (e) (see the color legends in each panel). The solid lines show the borders between V1 and V2, which correspond to the representation of the vertical meridian, in the lower visual field (upper border) and the upper visual field (lower border). The dotted line marks the fundus of the calcarine sulcus. Note that polar angle varies perpendicular to the border, whereas eccentricity varies with anterior-posterior position along the calcarine sulcus. CC, corpus callosum; CaS, calcarine sulcus; POS, parietal-occipital sulcus. (Modified from Wandell et al., 2007.)

A common feature of visual field maps, especially those in occipital areas, is a disproportionately large representation of the foveal region. This can be expressed in terms of a linear Cortical Magnification Factor (CMF)—the mm

of cortex per degree of visual angle—which shows a rapid decrease with increasing eccentricity (M. I. Sereno et al., 1995). Relative to owl monkeys and macaques, the change in CMF is much steeper in humans, suggesting a greater emphasis on foveal vision. This foveal bias partially reflects the greater density of cones in the fovea compared with the periphery, further exaggerated by later stages of processing in the retina and LGN, which oversample foveal signals (Connolly & Van Essen, 1984).

While a retinotopic reference frame is dominant in many visual areas, particularly in posterior parts of the brain, there is evidence for head- (Duhamel, Bremmer, BenHamed, & Graf, 1997; M. I. Sereno & Huang, 2006), body- (Makin, Holmes, & Zohary, 2007; Snyder, Grieve, Brotchie, & Andersen, 1998), and world-centered reference frames (Chafee, Averbeck, & Crowe, 2007; Snyder et al., 1998) in parietal cortex. How retinotopic input is transformed into these alternate reference frames remains unclear.

In summary, retinotopic or visual field maps are a common feature of visual cortex. Having described general features of visual cortex, the next sections will discuss the first two major visual cortical areas (V1 and V2) before turning to the major pathways of visual processing in cortex.

V1—PRIMARY VISUAL CORTEX

V1 is also known as striate cortex because of the prominent stripe of white matter (*stria Gennari*) running through layer 4. It is the largest single area in the cerebral cortex of the macaque (Felleman & Van Essen, 1991), occupying around 13% of the total cortical surface area (Sincich, Adams, & Horton, 2003). In humans, the fractional area of cortex occupied by V1 is only around 2% (Van Essen, 2004). However, the intrinsic shape of V1 in human and monkey is very similar (Hinds et al., 2008). V1 and V2 have a mirror-symmetric retinotopic organization with the vertical meridian represented along their common border (J. M. Allman & Kaas, 1974; M. I. Sereno et al., 1995). The upper field in V1 is represented ventrally and the lower visual field dorsally. In human, most of V1 is contained within the banks of the calcarine sulcus (Hinds et al., 2008; Rademacher, Caviness, Steinmetz, & Galaburda, 1993; Stensaas, Eddington, & Dobelle, 1974) (Figure 4.10).

Staining for cytochrome oxidase (CO), a mitochondrial enzyme indictaing the level of metabolic activity, reveals a distinctive pattern in V1 (Horton, 1984). Specifically, the CO density in each layer mirrors the strength of the input from the LGN with highest density in layers 2/3, 4C, 4A, and 6. Further, there is a regular pattern of dark patches ("blobs") interspersed with lighter areas (interpatches or interblobs) prominent in layers 2/3.

The three streams defined by the three major cell types in the LGN are maintained into V1 (Sincich & Horton, 2005a). The magnocellular layers of LGN project to layer 4Cα in V1, the parvocellular layers to layer 4Cβ, and the koniocellular layers to the CO rich blobs in layers 2 and 3, layer 1, and layer 4A (Hendry & Yoshioka, 1994). The magnocellular and parvocellular layers of LGN also provide input to layer 6. While early reports suggested that the different streams remained segregated even within V1, more recently it has become clear that there are extensive interactions between the streams beyond the input layer in V1 (Sincich & Horton, 2005a). For example, the blobs and interblobs in layer 2/3 receive input from the magnocellular and parvocellular recipient layers of V1 (Lachica, Beck, & Casagrande, 1992; Yabuta & Callaway, 1998) (Figure 4.11). However, some compartmentalization may still be maintained by specialized connectivity of cell types within laminae (for review, see Nassi & Callaway, 2009).

Visual input from the two eyes—segregated into separate layers in the LGN—remains segregated in layer 4C of V1 as alternating bands across the entire thickness of the cortex. These "ocular dominance columns" can be visualized in human with fMRI (Cheng, Waggoner, & Tanaka, 2001; Yacoub, Shmuel, Logothetis, & Ugurbil, 2007). The first intermixing of the inputs from the two eyes in visual processing occurs in the layers above and below layer 4 with neurons that respond better to binocular than monocular stimulation. These binocularly driven neurons are often sensitive to retinal disparity, the small geometric differences between the images in each eye (Cumming & Parker, 1999, 2000). Such sensitivity is necessary for stereopsis, the sense of depth (Ponce & Born, 2008).

Neurons in V1 also show selectivity for color, direction, and orientation. While neurons in the input layers of V1 have similar center-surround receptive fields to those observed in LGN, in other layers, receptive fields become elongated, responding strongly to oriented bars. "Simple cells" have receptive fields consisting of distinct excitatory and inhibitory subregions, whereas "complex cells" have subregions that are intermixed (Hubel & Wiesel, 1968). This difference between simple and complex cells may reflect underlying differences in spike threshold (Priebe, Mechler, Carandini, & Ferster, 2004).

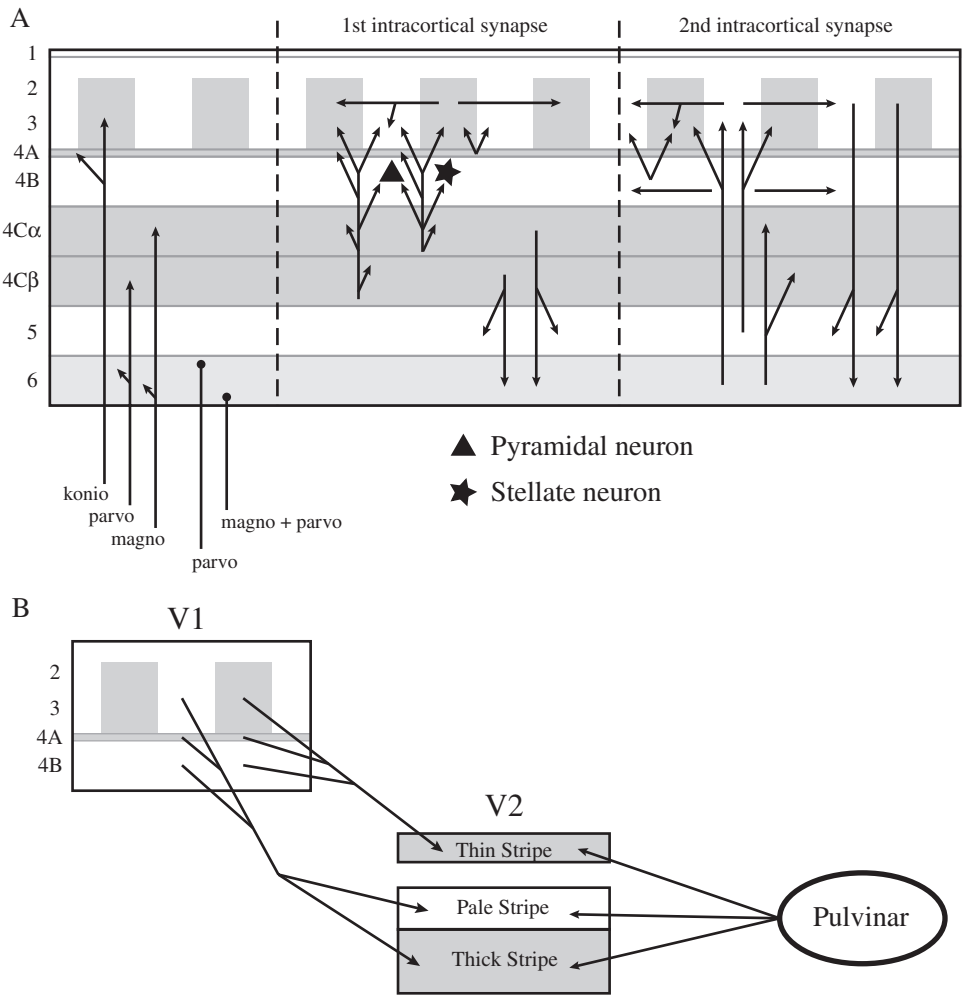

Figure 4.11 Connections of V1. (A) Intracortical connections of V1. After the initial input to V1 from the LGN, there is substantial mixing of the signals from the magnocellular, parvocellular, and koniocellular layers with common projections into layers 2/3 and an increasing emphasis on horizontal projections. (B) Projections from V1 to V2. There are two major pathways: (1) CO blobs (patches) → thin stripe, and (2) interblobs (interpatches) → pale and thick stripes. The pulvinar projections to V2 are complementary to those from V1 and may account for the different CO staining of the thick and pale stripes. In addition to projections from layers 2/3, 4A, and 4B, there are some projections from layers 5 and 6 (not shown). (Modified from Sincich & Horton, 2005a.)

A simple feedforward model of V1 simple cells proposed that each simple cell gets its input from an array of LGN center-surround receptive fields arranged along a straight line in visual space (Hubel & Wiesel, 1962). While this model has held up well, it is debated whether feedback in the form of lateral inhibition is also needed to explain the response properties of V1 neurons and in particular the sharpness of tuning (Priebe & Ferster, 2008; Shapley, Hawken, & Xing, 2007).

There is a columnar organization for orientation preference in V1. Columns run perpendicular to the cortical surface and neurons within a given column share the same orientation selectivity and have receptive fields in the same part of the visual field. Along the cortical surface all orientations are represented. Further, at points where neurons with different orientations meet, a characteristic pinwheel pattern is formed (Obermayer & Blasdel, 1993) with a center that tends to occur near the center of an ocular dominance patch.

Although orientation columns are much smaller then the size of standard voxels in fMRI experiments, it has been demonstrated that orientation can be decoded from the response across human V1 (Haynes & Rees, 2005; Kamitani & Tong, 2005). While this could in principle

reflect local biases in the orientation column sampling of individual voxels, suggesting that fMRI can be sensitive to subvoxel information, it more likely reflects a large-scale orientation map in human cortex (Freeman, Brouwer, Heeger, & Merriam, 2011; Sasaki et al., 2006).

Many V1 neurons are color-selective and some of these show no orientation selectivity (E. N. Johnson, Hawken, & Shapley, 2001). However, the organization of color selectivity in V1 has been the source of controversy over two issues (for review, see Sincich & Horton, 2005a). First, it has been debated whether color and orientation selectivity are segregated in V1 with some groups finding evidence in favor of segregation (e.g., Livingstone & Hubel, 1984) and others not (e.g., Leventhal, Thompson, Liu, Zhou, & Ault, 1995). Second, it has been debated whether color selectivity aligns specifically with blobs, with some groups finding close correspondence (Tootell, Silverman, Hamilton, De Valois, & Switkes, 1988) and others not (Landisman & Ts'o, 2002a, 2002b). While these debates may not be fully resolved, a recent study using intrinsic optical imaging reported both good alignment between color blobs and CO blobs and also low orientation selectivity within color blobs (Lu & Roe, 2008).

In summary, V1 receives input from the LGN in three streams (magnocellular, parvocellular, and magnocellular) segregated by eye. Within V1, the signals from the two eyes come together, the response properties of neurons become more complex than those observed at earlier levels of visual processing and there is some mixing of signals from the three streams. The major output of V1 is to V2, the focus of the next section.

V2

V2 is smaller then V1, but still occupies around 10% of the total cortical surface area in macaques (Sincich et al., 2003). CO staining in V2 reveals a pattern of stripes perpendicular to the V1 border (Horton, 1984; Tootell, Silverman, De Valois, & Jacobs, 1983) consisting of thick and thin dark stripes interleaved by pale thin stripes. Neurons in the different V2 stripes differ in their physiological properties (e.g., G. Chen, Lu, & Roe, 2008; DeYoe & Van Essen, 1985; Hubel & Livingstone, 1987; Lu & Roe, 2008; Shipp & Zeki, 2002a) and there appear to be separate visual field maps for each stripe type (Roe & Ts'o, 1995; Shipp & Zeki, 2002b). Early studies suggested that three functional streams were maintained from V1 to V2 with (1) the blobs in layer 2/3 in V1 projecting to the thin stripes, (2) the inter-blobs projecting to the pale stripes, and (3) layer 4B projecting to the thick stripes. These three streams were proposed to contribute to color, form, and motion/depth processing, respectively (M. Livingstone & Hubel, 1988). However, more recent studies have revealed greater intermixing between the projections from V1 (Sincich & Horton, 2002a) with just two major streams (Figure 4.11). First, the blobs in layer 2/3 project to the thin stripes (Sincich & Horton, 2005b) but there are also some projections from cells in other layers (Sincich, Jocson, & Horton, 2007). Second, the interblobs in layer 2/3, as well as cells in layers 4A, 4B, and 5/6, project to both the thick stripes and the pale stripes (Sincich & Horton, 2002a; Sincich, Jocson, & Horton, 2010). The different CO staining for thick and pale stripes despite their similar input may reflect different contributions from the pulvinar (Sincich & Horton, 2002b). There is also extensive feedback from V2 to V1, but organization of feedback projections with respect to the blobs and interblobs is unclear (Shmuel et al., 2005; Stettler, Das, Bennett, & Gilbert, 2002).

Like V1, V2 contains orientation- (Hubel & Wiesel, 1970; Levitt, Kiper, & Movshon, 1994; S. M. Zeki, 1978) and direction-selective neurons (Burkhalter & Van Essen, 1986), although the receptive fields are larger in V2 (Gattass, Gross, & Sandell, 1981; Smith, Singh, Williams, & Greenlee, 2001). Many neurons are selective for stimulus color (Burkhalter & Van Essen, 1986; Levitt et al., 1994) and there are a greater proportion of color-oriented neurons compared with V1 (A.W. Roe & Ts'o, 1997). There appears to be some segregation of neurons with selective responses to color, size, and motion between the different stripes in V2, consistent with some continued separation of parvocellular and magnocellular pathways, although this segregation is not absolute and all neuron types are found in all stripes (Levitt et al., 1994). However, direction-selective neurons are most prominent in thick stripes with direction maps reported in thick and pale stripes (Lu, Chen, Tanigawa, & Roe, 2010), thin stripes appear to contain a hue map (Lim, Wang, Xiao, Hu, & Felleman, 2009; Xiao, Wang, & Felleman, 2003), and orientation selectivity is strongest in thick and pale stripes (Sincich & Horton, 2005a).

V2 is thought to play a critical role in binocular depth perception (for reviews, see Cumming & DeAngelis, 2001; Parker, 2007). Most V2 neurons are binocularly driven and like V1 many are selective for retinal disparity (Hubel & Livingstone, 1987). However, tuning for disparity is very different in V1 and V2. When assessing depth of objects, human observers rely on relative disparity more than absolute disparity (e.g., Westheimer,

1979) and neurons in V2 show consistent selectivity for relative disparity (Thomas, Cumming, & Parker, 2002). In contrast, V1 neurons are selective for absolute disparity only (Cumming & Parker, 1999).

While simple orientation selectivity is common in V2, many neurons respond better to more complex visual stimuli such as angles, curves, intersecting lines, and complex gratings (e.g., polar and concentric) (Hegde & Van Essen, 2000; Ito & Komatsu, 2004; Mahon & De Valois, 2001). Further, while around 70% of V2 neurons show consistent orientation selectivity across locations within the receptive field, many others exhibit subregions within the receptive fields selective for different orientations (Figure 4.12), suggesting coding of combinations of orientations (Anzai, Peng, & Van Essen, 2007). V2 neurons are also responsive to illusory (von der Heydt, Peterhans, & Baumgartner, 1984) and texture-defined (von der Heydt & Peterhans, 1989) contours and to border ownership (which side of a contour is figure and which is ground) (Zhou, Friedman, & von der Heydt, 2000). Analysis of V2 neuronal response during viewing of natural images (Willmore, Prenger, & Gallant, 2010) suggests that V2 contains two distinct subpopulations: one with properties similar to those observed in V1, and one with more complex properties, exhibiting

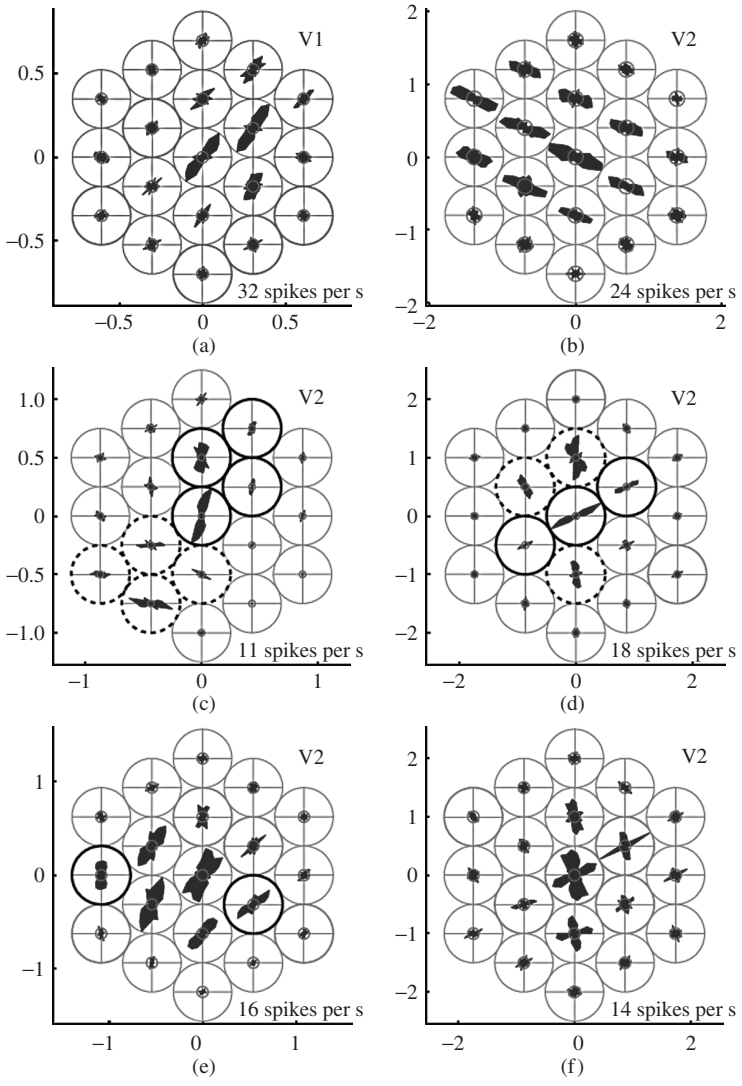

Figure 4.12 Orientation subregions within V2 receptive fields. (Color image on page C2.) Responses (filled blue curves) of macaque neurons relative to mean firing rates (red circles) plotted in polar coordinates as a function of stimulus orientation. The gray circles show the locations tested and the radius of the circle corresponds to the maximum firing rate observed (numbers on lower right corner of each map). Solid and dashed black lines highlight subregions tuned to different orientations. (a) V1 neuron with uniform tuning. V1 neurons showed minimal variation in tuning. (b) V2 neuron with uniform tuning. (c–f) V2 neurons showing nonuniform tuning with different orientation preferences in different locations (c–e) or bimodal tuning (f). (Modified from Anzai et al., 2007.)

strong suppressive tuning. Whether any of these functional differences correlate with the anatomical structure of V2 remains to be determined.

In summary, V2 receives strong input from V1. Mixing of the parvo-, magno-, and koniocellular pathways in V1 and in the projections from V1 and V2 makes it hard to assess the distinct contributions of these pathways. However, the presence of some functional clustering by, for example, color and direction-selectivity, suggests that there may still be some separation between the signals originating from the different LGN layers that may further influence the next stages of processing.

MAJOR CORTICAL VISUAL PROCESSING PATHWAYS

A key framework that has guided visual neuroscience is the division of cortical visual processing into distinct ventral and dorsal pathways (Mishkin, Ungerleider, & Macko, 1983; Ungerleider & Mishkin, 1982). Both pathways originate in V1, with the ventral pathway coursing through occipitotemporal cortex into the temporal lobe and the dorsal pathway coursing through occipitoparietal cortex into the posterior parietal cortex. Lesions of the ventral pathway in monkey produced selective deficits in object discrimination, leading to its characterization as a "What" pathway. Conversely, lesions of the dorsal pathway produced selective deficits in visuospatial tasks, leading to its characterization as a "Where" pathway. Further, the dorsal and ventral pathways were found to extend into dorsolateral prefrontal cortex and ventrolateral prefrontal cortex, respectively (Macko et al., 1982). Subsequently, a patient (D.F.) (Milner et al., 1991) with a large bilateral lesion of the occipitotemporal cortex and mostly spared occipitoparietal cortex (James, Culham, Humphrey, Milner, & Goodale, 2003), was found to have impaired perception of objects (agnosia) but intact ability to reach for objects, including shaping her grasping hand to reflect the size, shape, and orientation of an object (Milner et al., 1991). Further, while D.F. could not adjust the orientation of her hand to match the orientation of a distant slot, she could orient her hand appropriately when posting a card through the slot (Goodale, Milner, Jakobson, & Carey, 1991). These findings combined with the dense interconnections between the posterior parietal and premotor areas in frontal regions (Gentilucci & Rizzolatti, 1990) led to the proposal that the dorsal stream was more appropriately characterized as a "How" than as a "Where" pathway (Milner & Goodale, 2006). More recently, it has been proposed that neither "Where" nor "How" are sufficient to adequately capture the diversity of visuospatial functions supported by this pathway and that instead the dorsal pathway should be viewed as a neural nexus of visuospatial processing giving rise to at least three distinct pathways: parieto-prefrontal, parieto-premotor, and parieto-medial temporal, which primarily support spatial working memory, visually guided action, and spatial navigation, respectively (Kravitz, Saleem, Baker, & Mishkin, 2011).

In monkey, the segregation into ventral and dorsal pathways becomes most pronounced after initial processing in V1, V2, and V3. The ventral pathway emerges from these areas to include V4 and the inferior temporal (IT) cortex. The dorsal pathway projects from V1, V2, and V3 to MT and other areas in the parietal cortex. There are both direct projections as well as indirect projections via V6 in the anterior wall of the parieto-occipital sulcus (Fattori, Pitzalis, & Galletti, 2009; Galletti et al., 2001). Parietal and superior temporal areas within the dorsal pathway, including MT and the Lateral Intraparietal (LIP) area, are heavily interconnected with each other.

In the following sections, some of the major characteristics and functional properties of regions within both the ventral and dorsal pathways will be discussed.

VENTRAL PATHWAY

There are two striking functional properties that vary with the progression along the ventral pathway: size of receptive fields and complexity of stimuli required to elicit a response (Kobatake & Tanaka, 1994; Rousselet, Thorpe, & Fabre-Thorpe, 2004; Rust & Dicarlo, 2010). At the anterior end of the ventral pathway, neurons respond to complex stimuli within receptive fields much larger than those found in V1 and V2. These properties are consistent with a processing stream that is involved in object recognition, producing specific representations of objects or object features that are abstracted away from the spatial structure of the input at the retina (DiCarlo & Cox, 2007).

Position Tolerance

One of the biggest challenges faced by the visual system is to enable rapid and accurate object processing despite vast

differences in the retinal projection of an object produced by changes in, for example, viewing angle, size, illumination or position in the visual field (DiCarlo & Cox, 2007; Edelman, 1999; Ullman, 1997). Such "tolerance" or "invariance" is often considered one of the key characteristics of object recognition (DiCarlo & Cox, 2007). Changes in position (translations) are among the simplest of these transformations, because only the retinal position of the projection of an object is affected, and not the projection itself. The increase in receptive field size along the ventral pathway has long been thought to reflect one way in which tolerance for changes in position of an object was achieved.

In V1, receptive fields are typically small ($\sim$1 degree of visual angle) becoming larger in V2 (Gattass et al., 1981) and V4 ($<$4 degrees) (Desimone & Schein, 1987; Gattass, Sousa, & Gross, 1988) with the largest receptive fields found in anterior IT cortex. Early studies of anterior IT cortex emphasized the presence of very large receptive fields ($>$ 20 degrees) (Desimone & Gross, 1979; Gross, Rocha-Miranda, & Bender, 1972; Richmond, Wurtz, & Sato, 1983) and a largely preserved stimulus preference within receptive fields (Ito, Tamura, Fujita, & Tanaka, 1995; Lueschow, Miller, & Desimone, 1994; Schwartz, Desimone, Albright, & Gross, 1983). Such properties are consistent with a visual representation that is largely divorced from the retinotopic nature of the input. However, more recent studies have reported the presence of small receptive fields even in anterior IT (DiCarlo & Maunsell, 2003; Logothetis, Pauls, & Poggio, 1995) and a systematic study reported a range of sizes from 2.8 to 26 degrees with a mean size of 10 degrees, and large variability in response within receptive fields. These findings are consistent with the report of retinotopic maps in human visual cortex anterior to V4 (Arcaro et al., 2009; Brewer et al., 2005; Larsson & Heeger, 2006). Even in anterior regions where there is currently no evidence for retinotopic maps, there is substantial position information available (Schwarzlose, Swisher, Dang, & Kanwisher, 2008) and the representation of complex visual stimuli may still be dependent on position in the visual field (Cichy, Chen, & Haynes, 2011; Kravitz, Kriegeskorte, & Baker, 2010). This conclusion is supported by behavioral studies suggesting that complete position invariance is never achieved (Afraz, Pashkam, & Cavanagh, 2010; Kravitz et al., 2010; Kravitz, Vinson, & Baker, 2008). Thus, while tolerance for changes in position increases along the ventral pathway (Rust & Dicarlo, 2010), visual object representations are never completely abstracted away from the spatial nature of the input on the retina.

Form Selectivity in Single Neurons

In monkeys, the increase in the complexity of the functional properties observed from V1 to V2 continues into V4, although some properties are similar between these areas (Hegde & Van Essen, 2007). Like V2, many neurons in V4 are selective for complex gratings (Gallant, Connor, Rakshit, Lewis, & Van Essen, 1996), direction of motion (Cheng, Hasegawa, Saleem, & Tanaka, 1994) and disparity (Hinkle & Connor, 2001), with stronger effects of relative disparity than V2 (Umeda, Tanabe, & Fujita, 2007). Selectivity for color is highly prevalent in V4 and it was initially characterized as a color-processing area (S. Zeki, 1983; S. M. Zeki, 1973). Recent work suggests there may be some segregation of color and orientation sensitivity within V4 (Conway, Moeller, & Tsao, 2007; Tanigawa, Lu, & Roe, 2010). In comparing responses along the ventral pathway, much work has focused on selectivity for stimulus form.

In V4, parametric variation of simple two-dimensional contours, varying in curvature and orientation, revealed selectivity for angles and curves oriented in a particular direction with a bias for convex over concave features (Pasupathy & Connor, 1999) and acute curvature (Carlson, Rasquinha, Zhang, & Connor, 2011) (Figure 4.13). Such selectivity is also observed when the contours form part of a complex shape boundary, with neurons responding, for example, whenever a shape contains a sharp convex contour pointing to the right, with little impact of other parts of the shape (Pasupathy & Connor, 2001). Given these discrete responses to parts of a shape, it is possible to reconstruct a presented shape from the population response in V4.

More anteriorly, one of the most striking early observations of IT cortex was the presence of selectivity for complex shapes, real world objects, and even faces and body parts (Bruce, Desimone, & Gross, 1981; Desimone, Albright, Gross, & Bruce, 1984; Gross et al., 1972; Perrett, Rolls, & Caan, 1982) (Figure 4.14). To determine the critical features necessary to elicit responses an early approach was to use stimulus reduction. Starting with a complex object, features were incrementally removed to determine the minimum features necessary to elicit a strong response. While simple features are often sufficient in V4 and posterior IT, more complex features are required in anterior IT cortex (Kobatake & Tanaka, 1994; Tanaka, Saito, Fukada, & Moriya, 1991; Tsunoda, Yamane, Nishizaki, & Tanifuji, 2001). In many cases the critical features correspond more to object parts than to whole objects.

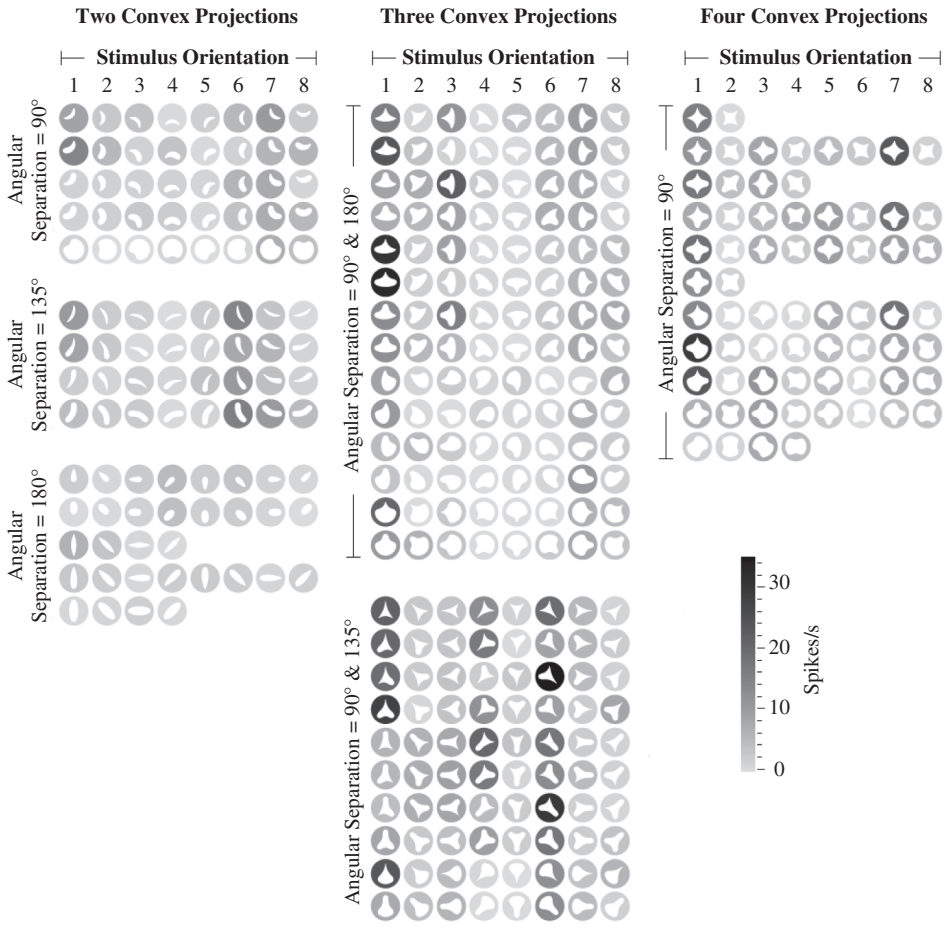

Figure 4.13 Position-specific tuning for boundaries in V4. Example V4 neuron in a macaque tuned for acute convex curvature near the top of the shape. Each circle corresponds to a single stimulus presented and the gray level surrounding each stimulus indicates the strength of response (see scale bar on right). (Modified from Pasupathy & Connor, 2002.)

Parametric variations of the dimensions of novel geometric stimuli in IT cortex have revealed selectivity for a variety of shape dimensions (Brincat & Connor, 2004; De Baene, Premereur, & Vogels, 2007; Kayaert, Biederman, Op de Beeck, & Vogels, 2005). In particular, neurons respond selectively to the presence of multiple two- or three-dimensional features with some neurons showing independent selectivity for separate features, as in V4, and others selectivity for specific multipart configurations (Brincat & Connor, 2004; Yamane, Carlson, Bowman, Wang, & Connor, 2008), which may increase with training (Baker, Behrmann, & Olson, 2002). This selectivity for complex configurations appears to evolve over the time course of the neural responses (Brincat & Connor, 2006).

As in V1, columnar organization has been reported in IT cortex (Fujita, Tanaka, Ito, & Cheng, 1992; Tanaka, 1996; Tsunoda et al., 2001) with each column representing particular types of object features. However, the organization may not be strictly columnar, but reflect the presence of some discrete clusters with neurons in each cluster sharing a limited degree of selectivity (Sato, Uchida, & Tanifuji, 2009).

Overall, single-unit recording studies in monkeys have highlighted an increase in stimulus selectivity of single neurons along the ventral visual pathway, with selectivity for complex features and even faces. In single neuron studies, it is difficult to determine the large-scale organization of stimulus selectivity in the cortex. fMRI, however, is ideal for investigating large-scale structure and one of the main characteristics revealed has been the presence of large regions with consistent patterns of selectivity.

Category Selectivity in fMRI

By contrasting responses to different categories of stimuli, human fMRI has revealed the presence of a limited (Downing, Chan, Peelen, Dodds, & Kanwisher, 2006) number of regions selective for particular categories, including faces

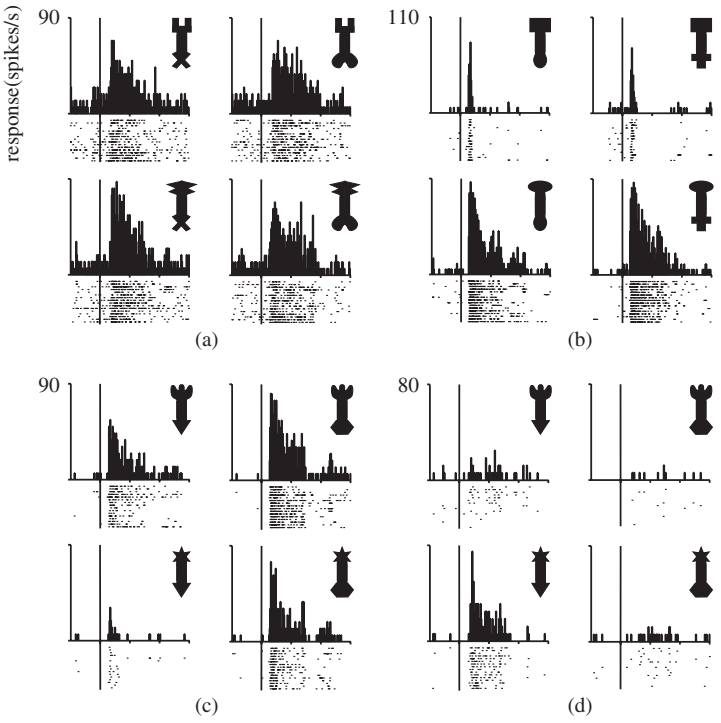

Figure 4.14 Example stimulus selectivity in inferior temporal cortex of the macaque. Response of four single inferior temporal neurons to baton stimuli composed of separate upper and lower parts. Responses are shown over 2,000 ms, aligned to stimulus onset (vertical line). Rasters show the firing of the neurons on individual trials and the histograms show the average firing rate across trials. (a) Neuron exhibiting no obvious selectivity with a strong visual response to all batons. (b) Neuron showing a strong response in the presence of the oval upper part, independent of the lower part. (c) Neuron with response modulated by both upper and lower parts. (d) Neuron responding only to a specific combination of upper and lower parts. Neurons showing this type of selectivity were more common for batons the monkey had been trained to discriminate. (Modified from from Baker, Behrmann, & Olson, 2002.)

(Kanwisher, McDermott, & Chun, 1997; Puce, Allison, Asgari, Gore, & McCarthy, 1996), objects (Kourtzi & Kanwisher, 2000; Malach et al., 1995), body parts (Downing, Jiang, Shuman, & Kanwisher, 2001; Peelen & Downing, 2007), scenes (Epstein & Kanwisher, 1998), and letter strings (Baker et al., 2007; Cohen & Dehaene, 2004; Puce et al., 1996) (Figure 4.15). Similar fMRI studies in monkeys have also revealed corresponding category-selective regions (Bell, Hadj-Bouziane, Frihauf, Tootell, & Ungerleider, 2009; Pinsk et al., 2009; Pinsk, DeSimone, Moore, Gross, & Kastner, 2005; Tsao, Freiwald, Knutsen, Mandeville, & Tootell, 2003; Tsao, Freiwald, Tootell, & Livingstone, 2006). For faces, six face-selective patches have been identified in the temporal lobe of the macaque (Moeller, Freiwald, & Tsao, 2008) (Figure 4.15). Critically, fMRI-guided single-unit recording studies within some of these patches have revealed that the vast majority of individual neurons are face-selective (Freiwald & Tsao, 2010; Tsao et al., 2006) although the information about faces appears to vary across patches (Freiwald & Tsao, 2010). Further, electrical stimulation within an individual face patch tends to elicit activation in the other patches (Moeller et al., 2008) suggesting that the patches may constitute a face-processing circuit (for discussion, see Baker, 2008). While these category-selective regions demonstrate clustering of neurons by selectivity, it is also clear that information is somewhat distributed throughout parts of the ventral stream with category-selective regions containing information about both preferred and nonpreferred categories (Haxby et al., 2001).

Support for the significance of category-selective regions comes from studies of individuals with brain damage to regions of the ventral pathway. Specific impairments have been reported for faces (e.g., Barton & Cherkasova, 2003), bodies (e.g., Moro et al., 2008), objects (e.g., Behrmann, Winocur, & Moscovitch, 1992), scenes (Aguirre & D'Esposito, 1999), and words (e.g., Mycroft, Behrmann, & Kay, 2009). Further, disrupting processing within category-selective regions using transcranial magnetic stimulation can produce specific deficits in the processing of those categories of visual stimuli (Pitcher, Charles, Devlin, Walsh, & Duchaine, 2009).

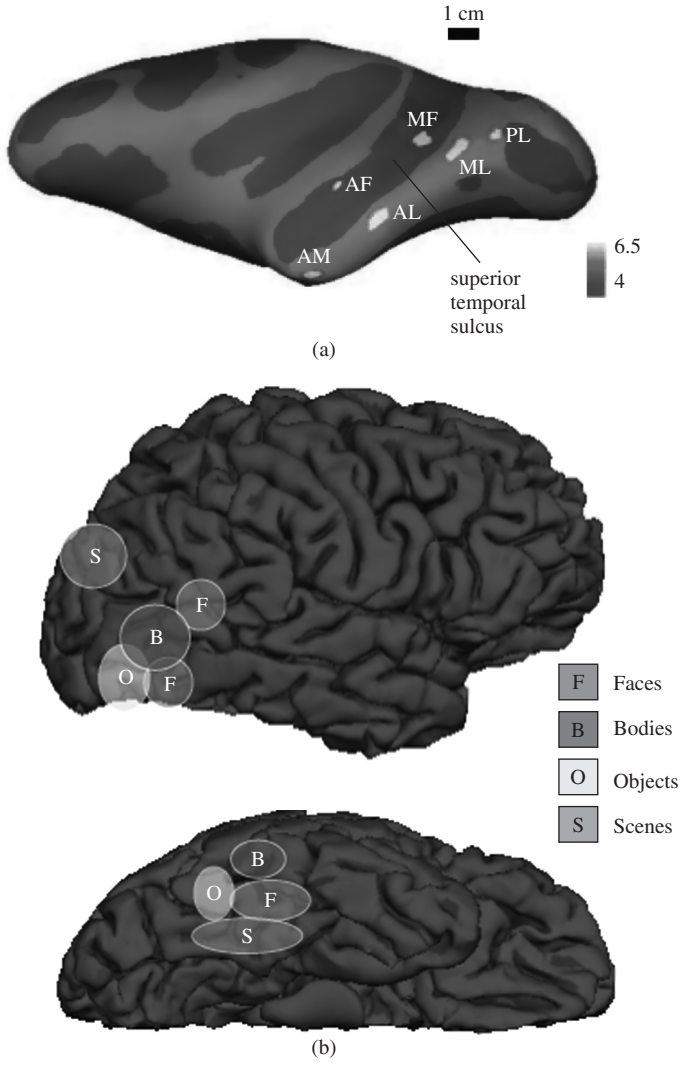

Figure 4.15 Category selectivity in monkey and human brain. (Color image on page C3.) (a) The six face patches that have been identified in monkey cortex by contrasting responses to faces with responses to objects. Patches are shown on an inflated hemisphere to show the depths of the sulci (modified from Freiwald & Tsao, 2010). (b) Locations of major category-selective regions in the human brain on both the lateral (upper) and ventral surface (lower).

Given these findings, does category define the organizational structure of the ventral pathway? As described earlier, full retinotopic maps have been described in posterior parts of the ventral stream (Arcaro et al., 2009; Brewer et al., 2005; Larsson & Heeger, 2006) as well as eccentricity biases along the ventral temporal cortex (Hasson, Levy, Behrmann, Hendler, & Malach, 2002; Levy, Hasson, Avidan, Hendler, & Malach, 2001), and it has been suggested that there might be a topography of simple shape features across IT cortex (Op de Beeck, Deutsch, Vanduffel, Kanwisher, & DiCarlo, 2008). One possibility is that the ventral pathway contains several overlapping maps for different stimulus dimensions and that category selectivity reflects the intersection of these maps producing complex and nonlinear response patterns across the cortex (Op de Beeck, Haushofer, & Kanwisher, 2008). Future work on the ventral pathway will need to address how category selectivity emerges from experience, whether it is composed of overlapping maps, and how this representational structure contributes to adaptive behavior.

DORSAL PATHWAY

While the ventral pathway is characterized by its selectivity for stimulus form, the prominent feature of the dorsal stream is selectivity for the spatial position of stimuli

and, in particular, the direction of visual motion. Further, regions within the dorsal pathway seem to play a particular role in the planning and execution of limb (for reviews, see Culham & Valyear, 2006; Milner & Goodale, 2006) and eye (e.g., Konen & Kastner, 2008) movements and posterior parietal cortex has been implicated in many aspects of attention (e.g., Medina et al., 2009; Shomstein & Behrmann, 2006) and other high-level cognitive functions (Culham & Kanwisher, 2001; J. Gottlieb & Snyder, 2010). The following sections will focus on two highly studied regions within the dorsal pathway, Middle Temporal Area (MT), and the Lateral Intraparietal area (LIP).

Middle Temporal Area (MT)

MT, sometimes referred to as V5 (S. Zeki, 2004), is a functionally and anatomically distinct area on the posterior bank of the superior temporal sulcus in monkey (Van Essen, Maunsell, & Bixby, 1981). Anatomically, it is characterized by direct inputs from V1 and heavy myelination. Functionally, it contains a representation of the contralateral visual field with a high concentration of direction-selective neurons (S. M. Zeki, 1974). In humans, MT can be localized with fMRI, based on its responsiveness to visual motion, to the posterior/dorsal limb of the inferior temporal sulcus (Dumoulin et al., 2000; Huk, Dougherty, & Heeger, 2002). However, it is difficult to separate human MT from adjacent regions based on functional properties alone and it is often referred to as hMT+.

The input to MT is typically regarded as being primarily magnocellular with direct and indirect projections from layer 4B in V1 (Figure 4.16), which receives most of its input from the magnocellular layers of the LGN via layer 4Cα of V1 (Fitzpatrick, Lund, & Blasdel, 1985; Yabuta, Sawatari, & Callaway, 2001). The V1 neurons that give rise to this MT projection are highly selective for motion direction (Movshon & Newsome, 1996). MT also receives indirect V1 input from V2 and V3. Importantly, the V1 neurons projecting directly to MT are distinct from those neurons projecting to V2 from the same layer (Sincich & Horton, 2003). There are also at least three nonmagnocellular inputs into MT. First, there is a direct LGN input from koniocellular neurons (Sincich, Park, Wohlgemuth, & Horton, 2004; Stepniewska, Qi, & Kaas, 1999). Second, there is a disynaptic input from parvocellular cells in the LGN via V1, which may involve the Meynert cells of layer 6 (Nassi, Lyon, & Callaway, 2006). Finally, there is a trisynaptic input from parvocellular cells via layer 4Cβ likely through the thick stripes of V2 (Nassi & Callaway, 2006).

Neurons in MT show selectivity for the direction, speed, and binocular disparity of moving visual stimuli with high-contrast sensitivity (for review, see Born & Bradley, 2005). There is some columnar organization by direction (Albright, Desimone, & Gross, 1984) and additional clustering according to disparity selectivity (DeAngelis & Newsome, 1999). The receptive fields of MT neurons are much larger than those in V1 and have strong suppressive surrounds, with similar direction and

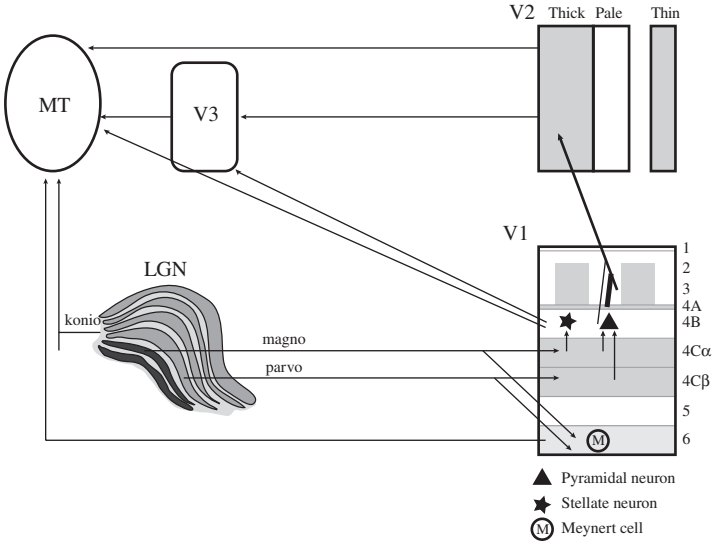

Figure 4.16 Pathways into MT. V1 provides the major input to MT with direct and indirect connections (via V2 and V3) dominated by magnocellular contributions. However, MT also receives direct input from koniocellular neurons in the LGN and disynaptic (via layer 6 in V1) and trisynaptic (via the thick stripes in V2) input from parvocellular cells. (Modified from Nassi & Callaway, 2006.)

disparity selectivity in the center and surround (J. Allman, Miezin, & McGuinness, 1985). This makes the neurons particularly sensitive to local changes in direction and depth, useful for figure-ground segregation. While surround suppression weakens sensitivity, the suppression is reduced when stimulus contrast is decreased (Pack, Hunter, & Born, 2005), suggesting dynamic modulation of sensitivity. However, reducing stimulus strength by reducing the coherence of motion stimuli has the opposite effect, increasing surround-suppression, suggesting that modulation of surround suppression is not a general response to noisy stimuli (Hunter & Born, 2011).

Importantly, the responses of MT cells can account for perceptual decisions about motion (Britten, Shadlen, Newsome, & Movshon, 1992; Newsome, Britten, & Movshon, 1989) and depth (Uka & DeAngelis, 2003, 2004). In some cases (Newsome et al., 1989; Uka & DeAngelis, 2003), but not all (J. Liu & Newsome, 2005), single neurons are found to be as sensitive as the observers. Further, judgments about motion-direction can be biased by electrical stimulation of MT (Salzman, Murasugi, Britten, & Newsome, 1992). These findings suggest a close link between the responses of MT neurons and the perception of motion.

Given the direct and indirect projects from V1, what is the role of these different projections? Reversible inactivation of V2 and V3 with cooling disrupts selectivity for binocular disparity more than selectivity for motion direction (Ponce, Lomber, & Born, 2008). This finding is consistent with the different disparity tuning in direction-selective V1 neurons compared with that in V2 and MT (Cumming & DeAngelis, 2001). In addition, cooling V2 and V3 shifts speed-tuning in MT toward slower speeds and slightly decreases surround suppression (Ponce, Hunter, Pack, Lomber, & Born, 2011). There was no evidence for patchy inputs of the projections from V2 and V3, suggesting that the indirect projections from V1 do not correspond directly with the functional organization observed.

In summary, MT receives the bulk of its input from V1, the first stage of cortical visual processing, and primarily encodes the motion information that contributes directly to motion perception. This motion information feeds forward into the rest of the dorsal stream contributing to visually guided action and spatial perception.

LATERAL INTRAPARIETAL AREA (LIP)

LIP, in the lateral wall of the monkey intraparietal sulcus, receives strong input from MT and is interconnected with the frontal eye field (FEF) and the superior colliculus (Blatt, Andersen, & Stoner, 1990). However, the putative human homologue of LIP is in the posterior medial, not lateral, intraparietal sulcus (Grefkes & Fink, 2005; Koyama et al., 2004). LIP contains a representation of the contralateral visual field, with receptive fields that are larger than MT and often centered around the fovea (Ben-Hamed, Duhamel, Bremmer, & Graf, 2001). Numerous single-unit and functional imaging studies have implicated LIP and the intraparieal sulcus in the control of attention and eye movements, but the precise function of LIP is unclear. The response properties observed are often complex and cannot be covered in detail here, but some of the major findings from monkeys are summarized below.

One theory about LIP is that it serves as a priority (or salience) map, reflecting the behavioral priority of stimuli in a spatial map, enabling the effective allocation of spatial attention (Bisley & Goldberg, 2010). Support for this view comes from data showing that responses in LIP appear to reflect the salience of stimuli within the receptive field (Balan & Gottlieb, 2006; Buschman & Miller, 2007; J. P. Gottlieb, Kusunoki, & Goldberg, 1998) and are modulated by task demands (e.g., Kusunoki, Gottlieb, & Goldberg, 2000; Mirpour, Arcizet, Ong, & Bisley, 2009).

Activity in LIP also reflects perceptual decisions (Gold & Shadlen, 2007). In tasks in which monkeys must evaluate a noisy stimulus (e.g., motion), activity in LIP gradually increases in those neurons representing the location of the chosen target, with the speed of increase correlating with the strength of the perceptual signal (Shadlen & Newsome, 2001) and evidence accumulation. Further, the time at which the neural activity reaches a critical level ("decision bound") reflects reaction time (Roitman & Shadlen, 2002) and may terminate the decision process (Kiani, Hanks, & Shadlen, 2008). The same neurons that accumulate evidence also appear to represent the confidence in the decision (Kiani & Shadlen, 2009).

LIP also plays a role in maintaining a stable representation of the visual world despite the constant eye movements we make. LIP neurons encode remembered locations (Gnadt & Andersen, 1988) and the spatial representation of those locations is dynamic, shifting to the corresponding retinal location around the time of a saccade (Duhamel, Colby, & Goldberg, 1992). Effectively, the retinal coordinates of stimuli are updated to anticipate the upcoming eye movement. This stimulus "remapping" (Hall & Colby, 2011) has also been observed in the human parietal cortex (Merriam, Genovese, & Colby, 2003) and in other monkey and human extrastriate areas

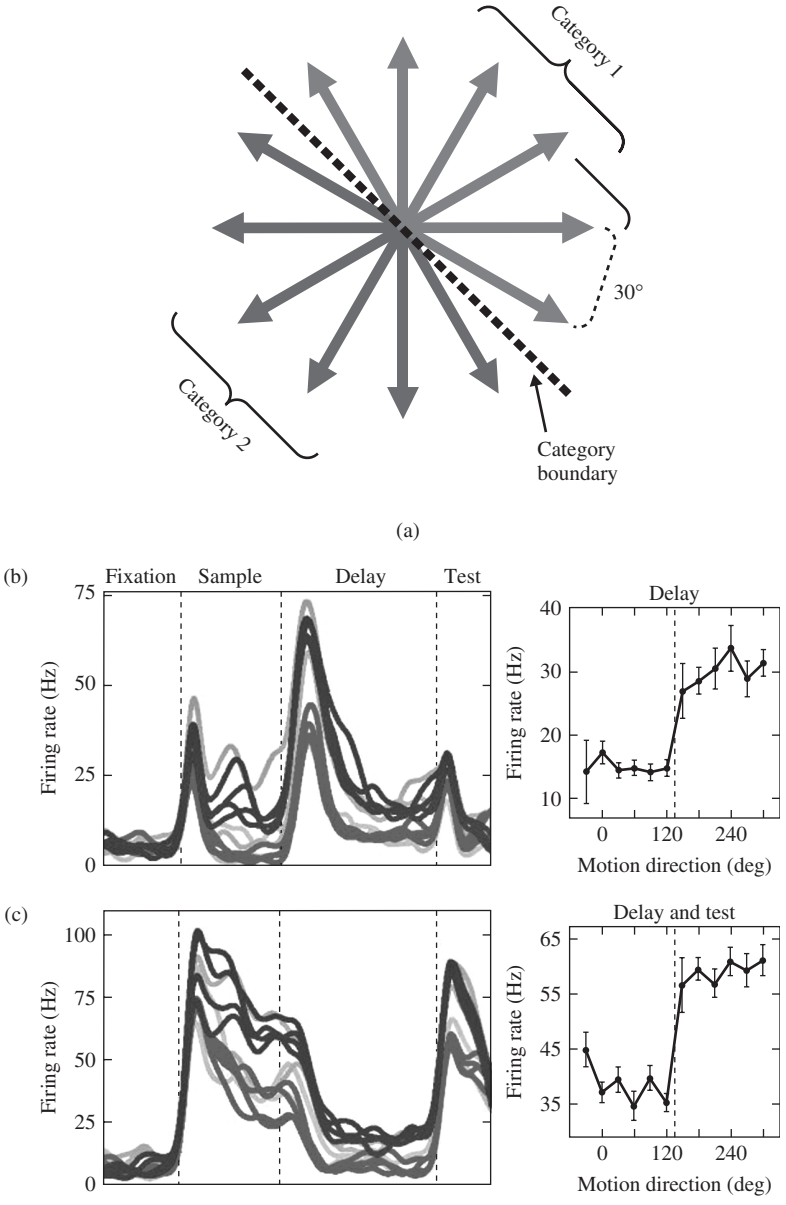

Figure 4.17 Category representations in LIP. (Color image on page C3.) (a) Monkeys were trained to group 12 possible motion directions into two categories (marked as red and blue) in a delayed-match-to-sample task. The black dotted line corresponds to the category boundary. (b) and (c) Responses to the 12 directions in two sample LIP neurons. The red and blue lines correspond to the two categories and pale lines correspond to the directions closest to the category boundary. The vertical dotted lines correspond to stimulus onset, stimulus offset and test-stimulus onset. The graphs on the right show the average responses to the 12 directions in either the delay period (a) or delay and test period (b). (Modified from Freedman & Assad, 2006.)

(Merriam, Genovese, & Colby, 2007; Nakamura & Colby, 2002).

Neurons in LIP also contain nonspatial information about stimulus attributes such as shape (A. B. Sereno & Maunsell, 1998), color (Toth & Assad, 2002) and numerosity (Roitman, Brannon, & Platt, 2007). In monkeys trained to categorize motion direction, responses in LIP, but not MT, reflected category information (Freedman & Assad, 2006) even when the stimuli were presented away from the cells receptive field (Freedman & Assad, 2009) (Figure 4.17).

Finally, given the varied functional properties that have been reported, it is worth noting that LIP in monkeys actually contains a dorsal and a ventral subdivision (Blatt et al., 1990) with different connectivity (Lewis & Van Essen, 2000; Medalla & Barbas, 2006) and some

distinct functional properties (Y. Liu, Yttri, & Snyder, 2010).

In summary, LIP exhibits complex response properties that differ substantially from those observed in MT, one of its major inputs. One of the challenges in characterizing the functional properties of LIP is to try and reconcile the diverse properties observed in these different, but well-defined and extensively studied tasks (e.g., Freedman & Assad, 2011).

CONCLUDING REMARKS

This chapter has surveyed visual processing in the primate from when light first enters the eye to the ends of the ventral and dorsal cortical visual processing pathways. A common theme highlighted throughout the different levels of processing, from the retina through to the cortex, is parallel processing in specialized cells or circuits. However, the segregation between different pathways is rarely complete and it is important not to oversimplify the complexity of visual processing. Through these diverging and converging pathways, the brain ultimately converts the patterns of light falling on the retina into representations of the visual world that are capable of supporting adaptive behaviors such as reaching and recognition of food, mates, and predators.

Three major aspects of visual processing were not covered in detail in this review. First, there is strong evidence that feedback plays a critical role in complex visual processing and awareness. For example, damage to the posterior parietal cortex can lead to hemispatial neglect, in which patients can neither attend to nor be aware of stimuli in one visual field. This deficit occurs despite the lack of damage to early visual areas or the ventral stream, speaking to the critical role of feedback and attention play in defining the contents of visual awareness. Further, the fact that feedback and attentional effects are found as early in the visual processing stream as the LGN, speaks to likely importance of these mechanisms in optimizing and modulating almost all levels of visual processing.

Second, from the retina through the cortex, processing is modified by experience and learning over many different timescales. Many neuronal properties, even in V1, such as orientation selectivity, directional selectivity, and ocular dominance, depend on visual experience early in life (first few months after birth) (Chiu & Weliky, 2004). Short-term exposure to a particular stimulus can produce perceptual after-effects, which are reflected in changes in cell responses for example, MT (Kohn & Movshon, 2004) and retina (Hosoya, Baccus, & Meister, 2005). Finally, long-term training with novel objects can shape the response properties in the IT cortex (Op de Beeck & Baker, 2010).

Finally, this chapter only considered the major visual pathways from the retina through LGN to the cortex. However, many other pathways contribute to visual processing, including, for example, several that pass through other nuclei of the thalamus (Wurtz, Joiner, & Berman, 2011), conveying internally generated information from other brain regions to areas of the visual cortex.

For many years, the macaque monkey has been the primary model of primate visual processing. As highlighted in this chapter, the advent of human fMRI has added a wealth of new information about visual processing in the human brain. However, one of the major areas of ignorance in human brain is connectivity. Developing techniques such as Diffusion Tensor Imaging (DTI) and the analysis of common slow fluctuations between brain regions (functional connectivity) promise to shed further light on the visual processing pathways in human.

REFERENCES

Afraz, A., Pashkam, M. V., & Cavanagh, P. (2010). Spatial heterogeneity in the perception of face and form attributes. *Current Biology, 20*(23), 2112–2116.

Aguirre, G. K., & D'Esposito, M. (1999). Topographical disorientation: A synthesis and taxonomy. *Brain, 122*(Pt 9), 1613–1628.

Ahmad, K. M., Klug, K., Herr, S., Sterling, P., & Schein, S. (2003). Cell density ratios in a foveal patch in macaque retina. *Visual Neuroscience, 20*(2), 189–209.

Albright, T. D., Desimone, R., & Gross, C. G. (1984). Columnar organization of directionally selective cells in visual area MT of the macaque. *Journal of Neurophysiology, 51*(1), 16–31.

Alitto, H. J., Moore, B. D., Rathbun, D. L., & Usrey, W. M. (2011). A comparison of visual responses in the lateral geniculate nucleus of alert and anaesthetized macaque monkeys. *Journal of Physiology, 589*(1), 87–99.

Alitto, H. J., & Usrey, W. M. (2008). Origin and dynamics of extraclassical suppression in the lateral geniculate nucleus of the macaque monkey. *Neuron, 57*(1), 135–146.

Allman, J., Miezin, F., & McGuinness, E. (1985). Direction- and velocity-specific responses from beyond the classical receptive field in the middle temporal visual area (MT). *Perception, 14*(2), 105–126.

Allman, J. M., & Kaas, J. H. (1974). The organization of the second visual area (V II) in the owl monkey: A second order transformation of the visual hemifield. *Brain Research, 76*(2), 247–265.

Anzai, A., Peng, X., & Van Essen, D. C. (2007). Neurons in monkey visual area V2 encode combinations of orientations. *Nature Neuroscience, 10*(10), 1313–1321.

Arcaro, M. J., McMains, S. A., Singer, B. D., & Kastner, S. (2009). Retinotopic organization of human ventral visual cortex. *Journal of Neuroscience, 29*(34), 10638–10652.

Arcaro, M. J., Pinsk, M. A., Li, X., & Kastner, S. (2011). Visuotopic organization of macaque posterior parietal cortex: A functional

magnetic resonance imaging study. *Journal of Neuroscience, 31*(6), 2064–2078.

Baker, C. I. (2008). Face to face with cortex. *Nature Neuroscience, 11*(8), 862–864.

Baker, C. I., Behrmann, M., & Olson, C. R. (2002). Impact of learning on representation of parts and wholes in monkey inferotemporal cortex. *Nature Neuroscience, 5*(11), 1210–1216.

Baker, C. I., Liu, J., Wald, L. L., Kwong, K. K., Benner, T., & Kanwisher, N. (2007). Visual word processing and experiential origins of functional selectivity in human extrastriate cortex. *Proceedings of the National Academy of Sciences, USA, 104*(21), 9087–9092.

Balan, P. F., & Gottlieb, J. (2006). Integration of exogenous input into a dynamic salience map revealed by perturbing attention. *Journal of Neuroscience, 26*(36), 9239–9249.

Barton, J. J., & Cherkasova, M. (2003). Face imagery and its relation to perception and covert recognition in prosopagnosia. *Neurology, 61*(2), 220–225.

Baylor, D. A., Lamb, T. D., & Yau, K. W. (1979). Responses of retinal rods to single photons. *Journal of Physiology, 288,* 613–634.

Baylor, D. A., Nunn, B. J., & Schnapf, J. L. (1987). Spectral sensitivity of cones of the monkey *Macaca fascicularis*. *Journal of Physiology, 390,* 145–160.

Behrmann, M., Winocur, G., & Moscovitch, M. (1992). Dissociation between mental imagery and object recognition in a brain-damaged patient. *Nature, 359*(6396), 636–637.

Bell, A. H., Hadj-Bouziane, F., Frihauf, J. B., Tootell, R. B., & Ungerleider, L. G. (2009). Object representations in the temporal cortex of monkeys and humans as revealed by functional magnetic resonance imaging. *Journal of Neurophysiology, 101*(2), 688–700.

BenHamed, S., Duhamel, J. R., Bremmer, F., & Graf, W. (2001). Representation of the visual field in the lateral intraparietal area of macaque monkeys: A quantitative receptive field analysis. *Experimental Brain Research, 140*(2), 127–144.

Berson, D. M. (2003). Strange vision: Ganglion cells as circadian photoreceptors. *Trends in Neurosciences, 26*(6), 314–320.

Bisley, J. W., & Goldberg, M. E. (2010). Attention, intention, and priority in the parietal lobe. *Annual Review of Neuroscience, 33,* 1–21.

Blasco, B., Avendano, C., & Cavada, C. (1999). A stereological analysis of the lateral geniculate nucleus in adult *Macaca nemestrina* monkeys. *Visual Neuroscience, 16*(5), 933–941.

Blatt, G. J., Andersen, R. A., & Stoner, G. R. (1990). Visual receptive field organization and cortico-cortical connections of the lateral intraparietal area (area LIP) in the macaque. *Journal of Comparative Neurology, 299*(4), 421–445.

Born, R. T., & Bradley, D. C. (2005). Structure and function of visual area MT. *Annual Review of Neuroscience, 28,* 157–189.

Boycott, B. B., & Wassle, H. (1991). Morphological classification of bipolar cells of the primate retina. *European Journal of Neuroscience, 3*(11), 1069–1088.

Brewer, A. A., Liu, J., Wade, A. R., & Wandell, B. A. (2005). Visual field maps and stimulus selectivity in human ventral occipital cortex. *Nature Neuroscience, 8*(8), 1102–1109.

Brewer, A. A., Press, W. A., Logothetis, N. K., & Wandell, B. A. (2002). Visual areas in macaque cortex measured using functional magnetic resonance imaging. *Journal of Neuroscience, 22*(23), 10416–10426.

Briggs, F., & Usrey, W. M. (2009). Parallel processing in the corticogeniculate pathway of the macaque monkey. *Neuron, 62*(1), 135–146.

Briggs, F., & Usrey, W. M. (2011). Corticogeniculate feedback and visual processing in the primate. *Journal of Physioliology, 589*(Pt 1), 33–40.

Brincat, S. L., & Connor, C. E. (2004). Underlying principles of visual shape selectivity in posterior inferotemporal cortex. *Nature Neuroscience, 7*(8), 880–886.

Brincat, S. L., & Connor, C. E. (2006). Dynamic shape synthesis in posterior inferotemporal cortex. *Neuron, 49*(1), 17–24.

Britten, K. H., Shadlen, M. N., Newsome, W. T., & Movshon, J. A. (1992). The analysis of visual motion: A comparison of neuronal and psychophysical performance. *Journal of Neuroscience, 12*(12), 4745–4765.

Bruce, C., Desimone, R., & Gross, C. G. (1981). Visual properties of neurons in a polysensory area in superior temporal sulcus of the macaque. *Journal of Neurophysiology, 46*(2), 369–384.

Bullier, J. (2004). Communications between cortical areas of the visual system. In L. M. Chalupa & J. S. Werner (Eds.), *The visual neurosciences* (Vol. 1). Cambridge, MA: MIT Press.

Burkhalter, A., & Van Essen, D. C. (1986). Processing of color, form and disparity information in visual areas VP and V2 of ventral extrastriate cortex in the macaque monkey. *Journal of Neuroscience, 6*(8), 2327–2351.

Buschman, T. J., & Miller, E. K. (2007). Top-down versus bottom-up control of attention in the prefrontal and posterior parietal cortices. *Science, 315*(5820), 1860–1862.

Buzas, P., Blessing, E. M., Szmajda, B. A., & Martin, P. R. (2006). Specificity of M and L cone inputs to receptive fields in the parvocellular pathway: Random wiring with functional bias. *Journal of Neuroscience, 26*(43), 11148–11161.

Calkins, D. J., & Sterling, P. (1999). Evidence that circuits for spatial and color vision segregate at the first retinal synapse. *Neuron, 24*(2), 313–321.

Carlson, E. T., Rasquinha, R. J., Zhang, K., & Connor, C. E. (2011). A sparse object coding scheme in area V4. *Current Biology, 21*(4), 288–293.

Casagrande, V. A., Sary, G., Royal, D., & Ruiz, O. (2005). On the impact of attention and motor planning on the lateral geniculate nucleus. *Progress in Brain Research, 149,* 11–29.

Chafee, M. V., Averbeck, B. B., & Crowe, D. A. (2007). Representing spatial relationships in posterior parietal cortex: Single neurons code object-referenced position. *Cerebral Cortex, 17*(12), 2914–2932.

Chan, T. L., Martin, P. R., Clunas, N., & Grunert, U. (2001). Bipolar cell diversity in the primate retina: Morphologic and immunocytochemical analysis of a new world monkey, the marmoset *Callithrix jacchus*. *Journal of Comparative Neurology, 437*(2), 219–239.

Chen, G., Lu, H. D., & Roe, A. W. (2008). A map for horizontal disparity in monkey V2. *Neuron, 58*(3), 442–450.

Chen, W., Zhu, X. H., Thulborn, K. R., & Ugurbil, K. (1999). Retinotopic mapping of lateral geniculate nucleus in humans using functional magnetic resonance imaging. *Proceedings of the National Academy of Sciences, USA, 96*(5), 2430–2434.

Cheng, K., Hasegawa, T., Saleem, K. S., & Tanaka, K. (1994). Comparison of neuronal selectivity for stimulus speed, length, and contrast in the prestriate visual cortical areas V4 and MT of the macaque monkey. *Journal of Neurophysiology, 71*(6), 2269–2280.

Cheng, K., Waggoner, R. A., & Tanaka, K. (2001). Human ocular dominance columns as revealed by high-field functional magnetic resonance imaging. *Neuron, 32*(2), 359–374.

Chiu, C., & Weliky, M. (2004). The role of neural activity in the development of orientation selectivity. In L. M. Chalupa & J. S. Werner (Eds.), *The visual neurosciences*. Cambridge, MA: MIT Press.

Cichy, R. M., Chen, Y., & Haynes, J. D. (2011). Encoding the identity and location of objects in human LOC. *Neuroimage, 54*(3), 2297–2307.

Cohen, L., & Dehaene, S. (2004). Specialization within the ventral stream: The case for the visual word form area. *Neuroimage, 22*(1), 466–476.

Connolly, M., & Van Essen, D. (1984). The representation of the visual field in parvicellular and magnocellular layers of the lateral

geniculate nucleus in the macaque monkey. *Journal of Comparative Neurology, 226*(4), 544–564.

Conway, B. R., Moeller, S., & Tsao, D. Y. (2007). Specialized color modules in macaque extrastriate cortex. *Neuron, 56*(3), 560–573.

Crook, J. D., Manookin, M. B., Packer, O. S., & Dacey, D. M. (2011). Horizontal cell feedback without cone type-selective inhibition mediates "red-green" color opponency in midget ganglion cells of the primate retina. *Journal of Neuroscience, 31*(5), 1762–1772.

Culham, J. C., & Kanwisher, N. G. (2001). Neuroimaging of cognitive functions in human parietal cortex. *Current Opinion in Neurobiology, 11*(2), 157–163.

Culham, J. C., & Valyear, K. F. (2006). Human parietal cortex in action. *Current Opinion in Neurobiology, 16*(2), 205–212.

Cumming, B. G., & DeAngelis, G. C. (2001). The physiology of stereopsis. *Annual Review of Neuroscience, 24,* 203–238.

Cumming, B. G., & Parker, A. J. (1999). Binocular neurons in V1 of awake monkeys are selective for absolute, not relative, disparity. *Journal of Neuroscience, 19*(13), 5602–5618.

Cumming, B. G., & Parker, A. J. (2000). Local disparity not perceived depth is signaled by binocular neurons in cortical area V1 of the Macaque. *Journal of Neuroscience, 20*(12), 4758–4767.

Curcio, C. A., & Allen, K. A. (1990). Topography of ganglion cells in human retina. *Journal of Comparative Neurology, 300*(1), 5–25.

Curcio, C. A., Sloan, K. R., Jr., Packer, O., Hendrickson, A. E., & Kalina, R. E. (1987). Distribution of cones in human and monkey retina: Individual variability and radial asymmetry. *Science, 236*(4801), 579–582.

Curcio, C. A., Sloan, K. R., Kalina, R. E., & Hendrickson, A. E. (1990). Human photoreceptor topography. *Journal of Comparative Neurology, 292*(4), 497–523.

Dacey, D. M. (2004). Origins of perception: Retinal ganglion cell diversity and the creation of parallel visual pathways. In M. S. Gazzaniga (Ed.), *The cognitive neurosciences* (pp. 281–301). Cambridge, MA: MIT Press.

Dacey, D. M., Liao, H. W., Peterson, B. B., Robinson, F. R., Smith, V. C., Pokorny, J., . . . Gamlin, P. D. (2005). Melanopsin-expressing ganglion cells in primate retina signal colour and irradiance and project to the LGN. *Nature, 433*(7027), 749–754.

Dacey, D. M., Peterson, B. B., Robinson, F. R., & Gamlin, P. D. (2003). Fireworks in the primate retina: In vitro photodynamics reveals diverse LGN-projecting ganglion cell types. *Neuron, 37*(1), 15–27.

De Baene, W., Premereur, E., & Vogels, R. (2007). Properties of shape tuning of macaque inferior temporal neurons examined using rapid serial visual presentation. *Journal of Neurophysiology, 97*(4), 2900–2916.

DeAngelis, G. C., & Newsome, W. T. (1999). Organization of disparity-selective neurons in macaque area MT. *Journal of Neuroscience, 19*(4), 1398–1415.

Deeb, S. S., Diller, L. C., Williams, D. R., & Dacey, D. M. (2000). Interindividual and topographical variation of L:M cone ratios in monkey retinas. *Journal of the Optical Society of America A. Optics, Image Science, and Vision, 17*(3), 538–544.

DeMonasterio, F. M., Schein, S. J., & McCrane, E. P. (1981). Staining of blue-sensitive cones of the macaque retina by a fluorescent dye. *Science, 213*(4513), 1278–1281.

Derrington, A. M., & Lennie, P. (1984). Spatial and temporal contrast sensitivities of neurones in lateral geniculate nucleus of macaque. *Journal of Physiology, 357,* 219–240.

Desimone, R., Albright, T. D., Gross, C. G., & Bruce, C. (1984). Stimulus-selective properties of inferior temporal neurons in the macaque. *Journal of Neuroscience, 4*(8), 2051–2062.

Desimone, R., & Gross, C. G. (1979). Visual areas in the temporal cortex of the macaque. *Brain Research, 178*(2–3), 363–380.

Desimone, R., & Schein, S. J. (1987). Visual properties of neurons in area V4 of the macaque: Sensitivity to stimulus form. *Journal of Neurophysiology, 57*(3), 835–868.

DeYoe, E. A., Carman, G. J., Bandettini, P., Glickman, S., Wieser, J., Cox, R., . . . Neitz, J. (1996). Mapping striate and extrastriate visual areas in human cerebral cortex. *Proceedings of the National Academy of Sciences, USA, 93*(6), 2382–2386.

DeYoe, E. A., & Van Essen, D. C. (1985). Segregation of efferent connections and receptive field properties in visual area V2 of the macaque. *Nature, 317*(6032), 58–61.

DiCarlo, J. J., & Cox, D. D. (2007). Untangling invariant object recognition. *Trends in Cognitive Sciences, 11*(8), 333–341.

DiCarlo, J. J., & Maunsell, J. H. (2003). Anterior inferotemporal neurons of monkeys engaged in object recognition can be highly sensitive to object retinal position. *Journal of Neurophysiology, 89*(6), 3264–3278.

Diller, L., Packer, O. S., Verweij, J., McMahon, M. J., Williams, D. R., & Dacey, D. M. (2004). L and M cone contributions to the midget and parasol ganglion cell receptive fields of macaque monkey retina. *Journal of Neuroscience, 24*(5), 1079–1088.

Dougherty, R. F., Koch, V. M., Brewer, A. A., Fischer, B., Modersitzki, J., & Wandell, B. A. (2003). Visual field representations and locations of visual areas V1/2/3 in human visual cortex. *Journal of Vision, 3*(10), 586–598.

Downing, P. E., Chan, A. W., Peelen, M. V., Dodds, C. M., & Kanwisher, N. (2006). Domain specificity in visual cortex. *Cerebral Cortex, 16*(10), 1453–1461.

Downing, P. E., Jiang, Y., Shuman, M., & Kanwisher, N. (2001). A cortical area selective for visual processing of the human body. *Science, 293*(5539), 2470–2473.

Duhamel, J. R., Bremmer, F., BenHamed, S., & Graf, W. (1997). Spatial invariance of visual receptive fields in parietal cortex neurons. *Nature, 389*(6653), 845–848.

Duhamel, J. R., Colby, C. L., & Goldberg, M. E. (1992). The updating of the representation of visual space in parietal cortex by intended eye movements. *Science, 255*(5040), 90–92.

Dumoulin, S. O., Bittar, R. G., Kabani, N. J., Baker, C. L., Jr., Le Goualher, G., Bruce Pike, G., & Evans, A. C. (2000). A new anatomical landmark for reliable identification of human area V5/MT: A quantitative analysis of sulcal patterning. *Cerebral Cortex, 10*(5), 454–463.

Edelman, S. (1999). *Representations and representation in vision*. Cambridge, MA: MIT Press.

Engel, S. A., Rumelhart, D. E., Wandell, B. A., Lee, A. T., Glover, G. H., Chichilnisky, E. J., & Shadlen, M. N. (1994). fMRI of human visual cortex. *Nature, 369*(6481), 525.

Epstein, R., & Kanwisher, N. (1998). A cortical representation of the local visual environment. *Nature, 392*(6676), 598–601.

Erisir, A., Van Horn, S. C., Bickford, M. E., & Sherman, S. M. (1997). Immunocytochemistry and distribution of parabrachial terminals in the lateral geniculate nucleus of the cat: A comparison with corticogeniculate terminals. *Journal of Comparative Neurology, 377*(4), 535–549.

Erisir, A., Van Horn, S. C., & Sherman, S. M. (1997). Relative numbers of cortical and brainstem inputs to the lateral geniculate nucleus. *Proceedings of the National Academy of Sciences, USA, 94*(4), 1517–1520.

Euler, T., Detwiler, P. B., & Denk, W. (2002). Directionally selective calcium signals in dendrites of starburst amacrine cells. *Nature, 418*(6900), 845–852.

Fattori, P., Pitzalis, S., & Galletti, C. (2009). The cortical visual area V6 in macaque and human brains. *Journal of Physiology Paris, 103*(1–2), 88–97.

Felleman, D. J., & Van Essen, D. C. (1991). Distributed hierarchical processing in the primate cerebral cortex. *Cerebral Cortex, 1*(1), 1–47.

Field, G. D., & Chichilnisky, E. J. (2007). Information processing in the primate retina: Circuitry and coding. *Annual Review of Neuroscience, 30,* 1–30.

Field, G. D., Gauthier, J. L., Sher, A., Greschner, M., Machado, T. A., Jepson, L. H., . . . Chichilnisky, E. J. (2010). Functional connectivity in the retina at the resolution of photoreceptors. *Nature, 467* (7316), 673–677.

Field, G. D., Sher, A., Gauthier, J. L., Greschner, M., Shlens, J., Litke, A. M., & Chichilnisky, E. J. (2007). Spatial properties and functional organization of small bistratified ganglion cells in primate retina. *Journal of Neuroscience, 27* (48), 13261–13272.

Fitzpatrick, D., Lund, J. S., & Blasdel, G. G. (1985). Intrinsic connections of macaque striate cortex: Afferent and efferent connections of lamina 4C. *Journal of Neuroscience, 5* (12), 3329–3349.

Fitzpatrick, D., Usrey, W. M., Schofield, B. R., & Einstein, G. (1994). The sublaminar organization of corticogeniculate neurons in layer 6 of macaque striate cortex. *Visual Neuroscience, 11* (2), 307–315.

Freedman, D. J., & Assad, J. A. (2006). Experience-dependent representation of visual categories in parietal cortex. *Nature, 443* (7107), 85–88.

Freedman, D. J., & Assad, J. A. (2009). Distinct encoding of spatial and nonspatial visual information in parietal cortex. *Journal of Neuroscience, 29* (17), 5671–5680.

Freedman, D. J., & Assad, J. A. (2011). A proposed common neural mechanism for categorization and perceptual decisions. *Nature Neuroscience, 14* (2), 143–146.

Freeman, J., Brouwer, G. J., Heeger, D. J., & Merriam, E. P. (2011). Orientation decoding depends on maps, not columns. *Journal of Neuroscience, 31* (13), 4792–4804.

Freiwald, W. A., & Tsao, D. Y. (2010). Functional compartmentalization and viewpoint generalization within the macaque face-processing system. *Science, 330* (6005), 845–851.

Fujita, I., Tanaka, K., Ito, M., & Cheng, K. (1992). Columns for visual features of objects in monkey inferotemporal cortex. *Nature, 360* (6402), 343–346.

Gallant, J. L., Connor, C. E., Rakshit, S., Lewis, J. W., & Van Essen, D. C. (1996). Neural responses to polar, hyperbolic, and Cartesian gratings in area V4 of the macaque monkey. *Journal of Neurophysiology, 76* (4), 2718–2739.

Galletti, C., Gamberini, M., Kutz, D. F., Fattori, P., Luppino, G., & Matelli, M. (2001). The cortical connections of area V6: An occipito-parietal network processing visual information. *European Journal of Neuroscience, 13* (8), 1572–1588.

Gattass, R., Gross, C. G., & Sandell, J. H. (1981). Visual topography of V2 in the macaque. *Journal of Comparative Neurology, 201* (4), 519–539.

Gattass, R., Sousa, A. P., & Gross, C. G. (1988). Visuotopic organization and extent of V3 and V4 of the macaque. *Journal of Neuroscience, 8* (6), 1831–1845.

Gauthier, J. L., Field, G. D., Sher, A., Greschner, M., Shlens, J., Litke, A. M., & Chichilnisky, E. J. (2009). Receptive fields in primate retina are coordinated to sample visual space more uniformly. *PLoS Biol, 7* (4), e1000063.

Gauthier, J. L., Field, G. D., Sher, A., Shlens, J., Greschner, M., Litke, A. M., & Chichilnisky, E. J. (2009). Uniform signal redundancy of parasol and midget ganglion cells in primate retina. *Journal of Neuroscience, 29* (14), 4675–4680.

Gentilucci, M., & Rizzolatti, G. (1990). Cortical Motor Control of Arm and Hand Movements. In M. A. Goodale (Ed.), *Vision and action: The control of grasping* (pp. 147–162). Norwood, NJ: Ablex.

Gnadt, J. W., & Andersen, R. A. (1988). Memory related motor planning activity in posterior parietal cortex of macaque. *Experimental Brain Research, 70* (1), 216–220.

Gold, J. I., & Shadlen, M. N. (2007). The neural basis of decision making. *Annual Review of Neuroscience, 30,* 535–574.

Gollisch, T., & Meister, M. (2010). Eye smarter than scientists believed: Neural computations in circuits of the retina. *Neuron, 65* (2), 150–164.

Goodale, M. A., Milner, A. D., Jakobson, L. S., & Carey, D. P. (1991). A neurological dissociation between perceiving objects and grasping them. *Nature, 349* (6305), 154–156.

Gooley, J. J., Lu, J., Fischer, D., & Saper, C. B. (2003). A broad role for melanopsin in nonvisual photoreception. *Journal of Neuroscience, 23* (18), 7093–7106.

Gottlieb, J., & Snyder, L. H. (2010). Spatial and nonspatial functions of the parietal cortex. *Current Opinion in Neurobiology, 20* (6), 731–740.

Gottlieb, J. P., Kusunoki, M., & Goldberg, M. E. (1998). The representation of visual salience in monkey parietal cortex. *Nature, 391* (6666), 481–484.

Grefkes, C., & Fink, G. R. (2005). The functional organization of the intraparietal sulcus in humans and monkeys. *Journal of Anatomy, 207* (1), 3–17.

Gross, C. G., Rocha-Miranda, C. E., & Bender, D. B. (1972). Visual properties of neurons in inferotemporal cortex of the macaque. *Journal of Neurophysiology, 35* (1), 96–111.

Hall, N. J., & Colby, C. L. (2011). Remapping for visual stability. *Philosophical Transactions of the Royal Society of London B: Biological Science, 366* (1564), 528–539.

Hasson, U., Levy, I., Behrmann, M., Hendler, T., & Malach, R. (2002). Eccentricity bias as an organizing principle for human high-order object areas. *Neuron, 34* (3), 479–490.

Hausselt, S. E., Euler, T., Detwiler, P. B., & Denk, W. (2007). A dendrite-autonomous mechanism for direction selectivity in retinal starburst amacrine cells. *PLoS Biology, 5* (7), e185.

Haxby, J. V., Gobbini, M. I., Furey, M. L., Ishai, A., Schouten, J. L., & Pietrini, P. (2001). Distributed and overlapping representations of faces and objects in ventral temporal cortex. *Science, 293* (5539), 2425–2430.

Haynes, J. D., & Rees, G. (2005). Predicting the orientation of invisible stimuli from activity in human primary visual cortex. *Nature Neuroscience, 8* (5), 686–691.

Hegde, J., & Van Essen, D. C. (2000). Selectivity for complex shapes in primate visual area V2. *Journal of Neuroscience, 20* (5), RC61.

Hegde, J., & Van Essen, D. C. (2007). A comparative study of shape representation in macaque visual areas v2 and v4. *Cerebral Cortex, 17* (5), 1100–1116.

Hendry, S. H., & Reid, R. C. (2000). The koniocellular pathway in primate vision. *Annual Review of Neuroscience, 23,* 127s–153.

Hendry, S. H., & Yoshioka, T. (1994). A neurochemically distinct third channel in the macaque dorsal lateral geniculate nucleus. *Science, 264* (5158), 575–577.

Hinds, O. P., Polimeni, J. R., Rajendran, N., Balasubramanian, M., Wald, L. L., Augustinack, J. C., . . . Schwartz, E. L. (2008). The intrinsic shape of human and macaque primary visual cortex. *Cerebral Cortex, 18* (11), 2586–2595.

Hinds, O. P., Rajendran, N., Polimeni, J. R., Augustinack, J. C., Wiggins, G., Wald, L. L., . . . Fischl, B. (2008). Accurate prediction of V1 location from cortical folds in a surface coordinate system. *Neuroimage, 39* (4), 1585–1599.

Hinkle, D. A., & Connor, C. E. (2001). Disparity tuning in macaque area V4. *Neuroreport, 12* (2), 365–369.

Hofer, H., Carroll, J., Neitz, J., Neitz, M., & Williams, D. R. (2005). Organization of the human trichromatic cone mosaic. *Journal of Neuroscience, 25* (42), 9669–9679.

Horton, J. C. (1984). Cytochrome oxidase patches: A new cytoarchitectonic feature of monkey visual cortex. *Philosophical Transactions of the Royal Society of London B: Biological Science, 304* (1119), 199–253.

Horton, J. C., & Hoyt, W. F. (1991). The representation of the visual field in human striate cortex: A revision of the classic Holmes map. *Archives of Ophthalmology, 109* (6), 816–824.

Hosoya, T., Baccus, S. A., & Meister, M. (2005). Dynamic predictive coding by the retina. *Nature, 436* (7047), 71–77.

Hubel, D. H., & Livingstone, M. S. (1987). Segregation of form, color, and stereopsis in primate area 18. *Journal of Neuroscience, 7* (11), 3378–3415.

Hubel, D. H., & Wiesel, T. N. (1962). Receptive fields, binocular interaction and functional architecture in the cat's visual cortex. *Journal of Physiology, 160,* 106–154.

Hubel, D. H., & Wiesel, T. N. (1968). Receptive fields and functional architecture of monkey striate cortex. *Journal of Physiology, 195* (1), 215–243.

Hubel, D. H., & Wiesel, T. N. (1970). Stereoscopic vision in macaque monkey: Cells sensitive to binocular depth in area 18 of the macaque monkey cortex. *Nature, 225* (5227), 41–42.

Hubel, D. H., & Wiesel, T. N. (1974). Uniformity of monkey striate cortex: A parallel relationship between field size, scatter, and magnification factor. *Journal of Comparative Neurology, 158* (3), 295–305.

Huk, A. C., Dougherty, R. F., & Heeger, D. J. (2002). Retinotopy and functional subdivision of human areas MT and MST. *Journal of Neuroscience, 22* (16), 7195–7205.

Hunter, J. N., & Born, R. T. (2011). Stimulus-dependent modulation of suppressive influences in MT. *Journal of Neuroscience, 31* (2), 678–686.

Ichida, J. M., & Casagrande, V. A. (2002). Organization of the feedback pathway from striate cortex (V1) to the lateral geniculate nucleus (LGN) in the owl monkey (*Aotus trivirgatus*). *Journal of Comparative Neurology, 454* (3), 272–283.

Irvin, G. E., Norton, T. T., Sesma, M. A., & Casagrande, V. A. (1986). W-like response properties of interlaminar zone cells in the lateral geniculate nucleus of a primate (*Galago crassicaudatus*). *Brain Research, 362* (2), 254–270.

Ito, M., & Komatsu, H. (2004). Representation of angles embedded within contour stimuli in area V2 of macaque monkeys. *Journal of Neuroscience, 24* (13), 3313–3324.

Ito, M., Tamura, H., Fujita, I., & Tanaka, K. (1995). Size and position invariance of neuronal responses in monkey inferotemporal cortex. *Journal of Neurophysiology, 73* (1), 218–226.

Jacoby, R., Stafford, D., Kouyama, N., & Marshak, D. (1996). Synaptic inputs to ON parasol ganglion cells in the primate retina. *Journal of Neuroscience, 16* (24), 8041–8056.

James, T. W., Culham, J., Humphrey, G. K., Milner, A. D., & Goodale, M. A. (2003). Ventral occipital lesions impair object recognition but not object-directed grasping: An fMRI study. *Brain, 126* (Pt 11), 2463–2475.

Johnson, E. N., Hawken, M. J., & Shapley, R. (2001). The spatial transformation of color in the primary visual cortex of the macaque monkey. *Nature Neuroscience, 4* (4), 409–416.

Johnson, K. O., & Hsiao, S. S. (1992). Neural mechanisms of tactual form and texture perception. *Annual Review of Neuroscience, 15,* 227–250.

Joo, H. R., Peterson, B. B., Haun, T. J., & Dacey, D. M. (2011). Characterization of a novel large-field cone bipolar cell type in the primate retina: Evidence for selective cone connections. *Visual Neuroscience, 28* (1), 29–37.

Kaas, J. H., Guillery, R. W., & Allman, J. M. (1972). Some principles of organization in the dorsal lateral geniculate nucleus. *Brain, Behavior, and Evolution, 6* (1), 253–299.

Kaas, J. H., & Hackett, T. A. (2000). Subdivisions of auditory cortex and processing streams in primates. *Proceedings of the National Academy of Sciences, USA, 97* (22), 11793–11799.

Kaas, J. H., & Huerta, M. F. (1988). The subcortical visual system of primates. In H. D. Steklis (Ed.), *Neurosciences. Vol. 4: Comparative primate biology* (pp. 327–391). New York, NY: Alan R. Liss.

Kamitani, Y., & Tong, F. (2005). Decoding the visual and subjective contents of the human brain. *Nature Neuroscience, 8* (5), 679–685.

Kanwisher, N., McDermott, J., & Chun, M. M. (1997). The fusiform face area: A module in human extrastriate cortex specialized for face perception. *Journal of Neuroscience, 17* (11), 4302–4311.

Kaplan, E., & Shapley, R. M. (1982). X and Y cells in the lateral geniculate nucleus of macaque monkeys. *Journal of Physiology, 330,* 125–143.

Kaplan, E., & Shapley, R. M. (1986). The primate retina contains two types of ganglion cells, with high and low contrast sensitivity. *Proceedings of the National Academy of Sciences, USA, 83* (8), 2755–2757.

Kastner, S., Schneider, K. A., & Wunderlich, K. (2006). Beyond a relay nucleus: Neuroimaging views on the human LGN. *Progress in Brain Research, 155,* 125–143.

Kayaert, G., Biederman, I., Op de Beeck, H. P., & Vogels, R. (2005). Tuning for shape dimensions in macaque inferior temporal cortex. *Eur Journal of Neuroscience, 22* (1), 212–224.

Kiani, R., Hanks, T. D., & Shadlen, M. N. (2008). Bounded integration in parietal cortex underlies decisions even when viewing duration is dictated by the environment. *Journal of Neuroscience, 28* (12), 3017–3029.

Kiani, R., & Shadlen, M. N. (2009). Representation of confidence associated with a decision by neurons in the parietal cortex. *Science, 324* (5928), 759–764.

Kobatake, E., & Tanaka, K. (1994). Neuronal selectivities to complex object features in the ventral visual pathway of the macaque cerebral cortex. *Journal of Neurophysiology, 71* (3), 856–867.

Kohn, A., & Movshon, J. A. (2004). Adaptation changes the direction tuning of macaque MT neurons. *Nature Neuroscience, 7* (7), 764–772.

Konen, C. S., & Kastner, S. (2008). Representation of eye movements and stimulus motion in topographically organized areas of human posterior parietal cortex. *Journal of Neuroscience, 28* (33), 8361–8375.

Kourtzi, Z., & Kanwisher, N. (2000). Cortical regions involved in perceiving object shape. *Journal of Neuroscience, 20* (9), 3310–3318.

Koyama, M., Hasegawa, I., Osada, T., Adachi, Y., Nakahara, K., & Miyashita, Y. (2004). Functional magnetic resonance imaging of macaque monkeys performing visually guided saccade tasks: Comparison of cortical eye fields with humans. *Neuron, 41* (5), 795–807.

Kravitz, D. J., Kriegeskorte, N., & Baker, C. I. (2010). High-level visual object representations are constrained by position. *Cerebral Cortex, 20* (12), 2916–2925.

Kravitz, D. J., Saleem, K. S., Baker, C. I., & Mishkin, M. (2011). A new neural framework for visuospatial processing. *Nature Reviews Neuroscience, 12* (4), 217–230.

Kravitz, D. J., Vinson, L. D., & Baker, C. I. (2008). How position dependent is visual object recognition? *Trends in Cognitive Sciences, 12* (3), 114–122.

Kuffler, S. W. (1953). Discharge patterns and functional organization of mammalian retina. *Journal of Neurophysiology, 16* (1), 37–68.

Kusunoki, M., Gottlieb, J., & Goldberg, M. E. (2000). The lateral intraparietal area as a salience map: The representation of abrupt onset, stimulus motion, and task relevance. *Vision Research, 40* (10–12), 1459–1468.

Lachica, E. A., Beck, P. D., & Casagrande, V. A. (1992). Parallel pathways in macaque monkey striate cortex: Anatomically defined columns in layer III. *?Proceedings of the National Academy of Sciences, USA, 89* (8), 3566–3570.

Landisman, C. E., & Ts'o, D. Y. (2002a). Color processing in macaque striate cortex: Electrophysiological properties. *Journal of Neurophysiology, 87* (6), 3138–3151.

Landisman, C. E., & Ts'o, D. Y. (2002b). Color processing in macaque striate cortex: Relationships to ocular dominance, cytochrome oxidase, and orientation. *Journal of Neurophysiology, 87* (6), 3126–3137.

Larsson, J., & Heeger, D. J. (2006). Two retinotopic visual areas in human lateral occipital cortex. *Journal of Neuroscience, 26*(51), 13128–13142.

Leventhal, A. G., Thompson, K. G., Liu, D., Zhou, Y., & Ault, S. J. (1995). Concomitant sensitivity to orientation, direction, and color of cells in layers 2, 3, and 4 of monkey striate cortex. *Journal of Neuroscience, 15*(3 Pt 1), 1808–1818.

Levitt, J. B., Kiper, D. C., & Movshon, J. A. (1994). Receptive fields and functional architecture of macaque V2. *Journal of Neurophysiology, 71*(6), 2517–2542.

Levy, I., Hasson, U., Avidan, G., Hendler, T., & Malach, R. (2001). Center-periphery organization of human object areas. *Nature Neuroscience, 4*(5), 533–539.

Lewis, J. W., & Van Essen, D. C. (2000). Corticocortical connections of visual, sensorimotor, and multimodal processing areas in the parietal lobe of the macaque monkey. *Journal of Comparative Neurology, 428*(1), 112–137.

Lim, H., Wang, Y., Xiao, Y., Hu, M., & Felleman, D. J. (2009). Organization of hue selectivity in macaque V2 thin stripes. *Journal of Neurophysiology, 102*(5), 2603–2615.

Liu, J., & Newsome, W. T. (2005). Correlation between speed perception and neural activity in the middle temporal visual area. *Journal of Neuroscience, 25*(3), 711–722.

Liu, Y., Yttri, E. A., & Snyder, L. H. (2010). Intention and attention: Different functional roles for LIPd and LIPv. *Nature Neuroscience, 13*(4), 495–500.

Livingstone, M., & Hubel, D. (1988). Segregation of form, color, movement, and depth: Anatomy, physiology, and perception. *Science, 240*(4853), 740–749.

Livingstone, M. S., & Hubel, D. H. (1984). Anatomy and physiology of a color system in the primate visual cortex. *Journal of Neuroscience, 4*(1), 309–356.

Logothetis, N. K., Pauls, J., & Poggio, T. (1995). Shape representation in the inferior temporal cortex of monkeys. *Current Biology, 5*(5), 552–563.

Lu, H. D., Chen, G., Tanigawa, H., & Roe, A. W. (2010). A motion direction map in macaque V2. *Neuron, 68*(5), 1002–1013.

Lu, H. D., & Roe, A. W. (2008). Functional organization of color domains in V1 and V2 of macaque monkey revealed by optical imaging. *Cerebral Cortex, 18*(3), 516–533.

Lueschow, A., Miller, E. K., & Desimone, R. (1994). Inferior temporal mechanisms for invariant object recognition. *Cerebral Cortex, 4*(5), 523–531.

Macko, K. A., Jarvis, C. D., Kennedy, C., Miyaoka, M., Shinohara, M., Sololoff, L., & Mishkin, M. (1982). Mapping the primate visual system with [2–14C]deoxyglucose. *Science, 218*(4570), 394–397.

MacNeil, M. A., Heussy, J. K., Dacheux, R. F., Raviola, E., & Masland, R. H. (1999). The shapes and numbers of amacrine cells: Matching of photofilled with Golgi-stained cells in the rabbit retina and comparison with other mammalian species. *Journal of Comparative Neurology, 413*(2), 305–326.

Mahon, L. E., & De Valois, R. L. (2001). Cartesian and non-Cartesian responses in LGN, V1, and V2 cells. *Visual Neuroscience, 18*(6), 973–981.

Makin, T. R., Holmes, N. P., & Zohary, E. (2007). Is that near my hand? Multisensory representation of peripersonal space in human intraparietal sulcus. *Journal of Neuroscience, 27*(4), 731–740.

Malach, R., Amir, Y., Harel, M., & Grinvald, A. (1993). Relationship between intrinsic connections and functional architecture revealed by optical imaging and in vivo targeted biocytin injections in primate striate cortex. *Proceedings of the National Academy of Sciences, USA, 90*(22), 10469–10473.

Malach, R., Reppas, J. B., Benson, R. R., Kwong, K. K., Jiang, H., Kennedy, W. A., . . . Tootell, R. B. (1995). Object-related activity revealed by functional magnetic resonance imaging in human occipital cortex. *Proceedings of the National Academy of Sciences, USA, 92*(18), 8135–8139.

Malpeli, J. G., & Baker, F. H. (1975). The representation of the visual field in the lateral geniculate nucleus of *Macaca mulatta*. *Journal of Comparative Neurology, 161*(4), 569–594.

Martin, P. R., & Grunert, U. (1999). Analysis of the short wavelength-sensitive ("blue") cone mosaic in the primate retina: Comparison of New World and Old World monkeys. *Journal of Comparative Neurology, 406*(1), 1–14.

Martin, P. R., Lee, B. B., White, A. J., Solomon, S. G., & Ruttiger, L. (2001). Chromatic sensitivity of ganglion cells in the peripheral primate retina. *Nature, 410*(6831), 933–936.

Masland, R. H. (2001a). The fundamental plan of the retina. *Nature Neuroscience, 4*(9), 877–886.

Masland, R. H. (2001b). Neuronal diversity in the retina. *Current Opinion in Neurobiology, 11*(4), 431–436.

McAlonan, K., Cavanaugh, J., & Wurtz, R. H. (2008). Guarding the gateway to cortex with attention in visual thalamus. *Nature, 456*(7220), 391–394.

Medalla, M., & Barbas, H. (2006). Diversity of laminar connections linking periarcuate and lateral intraparietal areas depends on cortical structure. *European Journal of Neuroscience, 23*(1), 161–179.

Medina, J., Kannan, V., Pawlak, M. A., Kleinman, J. T., Newhart, M., Davis, C., . . . Hillis, A. E. (2009). Neural substrates of visuospatial processing in distinct reference frames: Evidence from unilateral spatial neglect. *Journal of Cognitive Neuroscience, 21*(11), 2073–2084.

Melcher, D., & Colby, C. L. (2008). Trans-saccadic perception. *Trends in Cognitve Sciences, 12*(12), 466–473.

Merriam, E. P., Genovese, C. R., & Colby, C. L. (2003). Spatial updating in human parietal cortex. *Neuron, 39*(2), 361–373.

Merriam, E. P., Genovese, C. R., & Colby, C. L. (2007). Remapping in human visual cortex. *Journal of Neurophysiology, 97*(2), 1738–1755.

Milner, A. D., & Goodale, M. A. (2006). *The visual brain in action*. Oxford, UK: Oxford University Press.

Milner, A. D., Perrett, D. I., Johnston, R. S., Benson, P. J., Jordan, T. R., Heeley, D. W., . . . Davidson, D. L. W. (1991). Perception and action in "visual form agnosia." *Brain, 114*(Pt 1B), 405–428.

Mirpour, K., Arcizet, F., Ong, W. S., & Bisley, J. W. (2009). Been there, seen that: A neural mechanism for performing efficient visual search. *Journal of Neurophysiology, 102*(6), 3481–3491.

Mishkin, M., Ungerleider, L. G., & Macko, K. A. (1983). Object vision and spatial vision: 2 cortical pathways. *Trends in Neurosciences, 6*(10), 414–417.

Moeller, S., Freiwald, W. A., & Tsao, D. Y. (2008). Patches with links: A unified system for processing faces in the macaque temporal lobe. *Science, 320*(5881), 1355–1359.

Moro, V., Urgesi, C., Pernigo, S., Lanteri, P., Pazzaglia, M., & Aglioti, S. M. (2008). The neural basis of body form and body action agnosia. *Neuron, 60*(2), 235–246.

Movshon, J. A., & Newsome, W. T. (1996). Visual response properties of striate cortical neurons projecting to area MT in macaque monkeys. *Journal of Neuroscience, 16*(23), 7733–7741.

Mycroft, R. H., Behrmann, M., & Kay, J. (2009). Visuoperceptual deficits in letter-by-letter reading? *Neuropsychologia, 47*(7), 1733–1744.

Nakamura, K., & Colby, C. L. (2002). Updating of the visual representation in monkey striate and extrastriate cortex during saccades. *Proceedings of the National Academy of Sciences, USA, 99*(6), 4026–4031.

Nassi, J. J., & Callaway, E. M. (2006). Multiple circuits relaying primate parallel visual pathways to the middle temporal area. *Journal of Neuroscience, 26*(49), 12789–12798.

Nassi, J. J., & Callaway, E. M. (2009). Parallel processing strategies of the primate visual system. *Nature Reviews Neuroscience, 10*(5), 360–372.

Nassi, J. J., Lyon, D. C., & Callaway, E. M. (2006). The parvocellular LGN provides a robust disynaptic input to the visual motion area MT. *Neuron, 50*(2), 319–327.

Newsome, W. T., Britten, K. H., & Movshon, J. A. (1989). Neuronal correlates of a perceptual decision. *Nature, 341*(6237), 52–54.

O'Connor, D. H., Fukui, M. M., Pinsk, M. A., & Kastner, S. (2002). Attention modulates responses in the human lateral geniculate nucleus. *Nature Neuroscience, 5*(11), 1203–1209.

O'Shea, R. P. (1991). Thumb's rule tested: Visual angle of thumb's width is about 2 deg. *Perception, 20*(3), 415–418.

Obermayer, K., & Blasdel, G. G. (1993). Geometry of orientation and ocular dominance columns in monkey striate cortex. *Journal of Neuroscience, 13*(10), 4114–4129.

Okano, T., Kojima, D., Fukada, Y., Shichida, Y., & Yoshizawa, T. (1992). Primary structures of chicken cone visual pigments: Vertebrate rhodopsins have evolved out of cone visual pigments. *Proceedings of the National Academy of Sciences, USA, 89*(13), 5932–5936.

Olveczky, B. P., Baccus, S. A., & Meister, M. (2003). Segregation of object and background motion in the retina. *Nature, 423*(6938), 401–408.

Op de Beeck, H. P., & Baker, C. I. (2010). The neural basis of visual object learning. *Trends in Cognitive Sciences, 14*(1), 22–30.

Op de Beeck, H. P., Deutsch, J. A., Vanduffel, W., Kanwisher, N. G., & DiCarlo, J. J. (2008). A stable topography of selectivity for unfamiliar shape classes in monkey inferior temporal cortex. *Cerebral Cortex, 18*(7), 1676–1694.

Op de Beeck, H. P., Haushofer, J., & Kanwisher, N. G. (2008). Interpreting fMRI data: Maps, modules and dimensions. *Nature Reviews Neuroscience, 9*(2), 123–135.

Pack, C. C., Hunter, J. N., & Born, R. T. (2005). Contrast dependence of suppressive influences in cortical area MT of alert macaque. *Journal of Neurophysiology, 93*(3), 1809–1815.

Packer, O., Hendrickson, A. E., & Curcio, C. A. (1989). Photoreceptor topography of the retina in the adult pigtail macaque (*Macaca nemestrina*). *Journal of Comparative Neurology, 288*(1), 165–183.

Packer, O. S., Verweij, J., Li, P. H., Schnapf, J. L., & Dacey, D. M. (2010). Blue-yellow opponency in primate S cone photoreceptors. *Journal of Neuroscience, 30*(2), 568–572.

Parker, A. J. (2007). Binocular depth perception and the cerebral cortex. *Nature Reviews Neuroscience, 8*(5), 379–391.

Pasupathy, A., & Connor, C. E. (1999). Responses to contour features in macaque area V4. *Journal of Neurophysiology, 82*(5), 2490–2502.

Pasupathy, A., & Connor, C. E. (2001). Shape representation in area V4: Position-specific tuning for boundary conformation. *Journal of Neurophysiology, 86*(5), 2505–2519.

Peelen, M. V., & Downing, P. E. (2007). The neural basis of visual body perception. *Nature Reviews Neuroscience, 8*(8), 636–648.

Perrett, D. I., Rolls, E. T., & Caan, W. (1982). Visual neurones responsive to faces in the monkey temporal cortex. *Experimental Brain Research, 47*(3), 329–342.

Perry, V. H., Oehler, R., & Cowey, A. (1984). Retinal ganglion cells that project to the dorsal lateral geniculate nucleus in the macaque monkey. *Neuroscience, 12*(4), 1101–1123.

Peters, S., Heiduschka, P., Julien, S., Ziemssen, F., Fietz, H., Bartz-Schmidt, K. U., & Schraermeyer, U. (2007). Ultrastructural findings in the primate eye after intravitreal injection of bevacizumab. *American Journal of Ophthalmology, 143,* 995–1002.

Petrusca, D., Grivich, M. I., Sher, A., Field, G. D., Gauthier, J. L., Greschner, M., . . . Litke, A. M. (2007). Identification and characterization of a Y-like primate retinal ganglion cell type. *Journal of Neuroscience, 27*(41), 11019–11027.

Pinsk, M. A., Arcaro, M., Weiner, K. S., Kalkus, J. F., Inati, S. J., Gross, C. G. & Kastner, S. (2009). Neural representations of faces and body parts in macaque and human cortex: A comparative FMRI study. *Journal of Neurophysiology, 101*(5), 2581–2600.

Pinsk, M. A., DeSimone, K., Moore, T., Gross, C. G., & Kastner, S. (2005). Representations of faces and body parts in macaque temporal cortex: A functional MRI study. *Proceedings of the National Academy of Sciences, USA, 102*(19), 6996–7001.

Pitcher, D., Charles, L., Devlin, J. T., Walsh, V., & Duchaine, B. (2009). Triple dissociation of faces, bodies, and objects in extrastriate cortex. *Current Biology, 19*(4), 319–324.

Ponce, C. R., & Born, R. T. (2008). Stereopsis. *Current Biology, 18*(18), R845–850.

Ponce, C. R., Hunter, J. N., Pack, C. C., Lomber, S. G., & Born, R. T. (2011). Contributions of indirect pathways to visual response properties in macaque Middle Temporal Area MT. *Journal of Neuroscience, 31*(10), 3894–3903.

Ponce, C. R., Lomber, S. G., & Born, R. T. (2008). Integrating motion and depth via parallel pathways. *Nature Neuroscience, 11*(2), 216–223.

Priebe, N. J., & Ferster, D. (2008). Inhibition, spike threshold, and stimulus selectivity in primary visual cortex. *Neuron, 57*(4), 482–497.

Priebe, N. J., Mechler, F., Carandini, M., & Ferster, D. (2004). The contribution of spike threshold to the dichotomy of cortical simple and complex cells. *Nature Neuroscience, 7*(10), 1113–1122.

Przybyszewski, A. W., Gaska, J. P., Foote, W., & Pollen, D. A. (2000). Striate cortex increases contrast gain of macaque LGN neurons. *Visual Neuroscience, 17*(4), 485–494.

Puce, A., Allison, T., Asgari, M., Gore, J. C., & McCarthy, G. (1996). Differential sensitivity of human visual cortex to faces, letterstrings, and textures: A functional magnetic resonance imaging study. *Journal of Neuroscience, 16*(16), 5205–5215.

Rademacher, J., Caviness, V. S., Jr., Steinmetz, H., & Galaburda, A. M. (1993). Topographical variation of the human primary cortices: Implications for neuroimaging, brain mapping, and neurobiology. *Cerebral Cortex, 3*(4), 313–329.

Reid, R. C., & Shapley, R. M. (2002). Space and time maps of cone photoreceptor signals in macaque lateral geniculate nucleus. *Journal of Neuroscience, 22*(14), 6158–6175.

Richmond, B. J., Wurtz, R. H., & Sato, T. (1983). Visual responses of inferior temporal neurons in awake rhesus monkey. *Journal of Neurophysiology, 50*(6), 1415–1432.

Rockland, K. S., & Lund, J. S. (1983). Intrinsic laminar lattice connections in primate visual cortex. *Journal of Comparative Neurology, 216*(3), 303–318.

Rockland, K. S., & Pandya, D. N. (1979). Laminar origins and terminations of cortical connections of the occipital lobe in the rhesus monkey. *Brain Research, 179*(1), 3–20.

Rodieck, R. W., & Watanabe, M. (1993). Survey of the morphology of macaque retinal ganglion cells that project to the pretectum, superior colliculus, and parvicellular laminae of the lateral geniculate nucleus. *Journal of Comparative Neurology, 338*(2), 289–303.

Roe, A. W., & Ts'o, D. Y. (1995). Visual topography in primate V2: Multiple representation across functional stripes. *Journal of Neuroscience, 15*(5 Pt 2), 3689–3715.

Roe, A. W., & Ts'o, D. Y. (1997). The functional architecture of area V2 in the macaque monkey: Physiology, topography, connectivity. In K. S. Rockland, J. H. Kaas & A. Peters (Eds.), *Cerebral Cortex: Vol. 12. Extrastriate cortex in primates* (pp. 295–333). New York, NY: Plenum Press.

Roitman, J. D., Brannon, E. M., & Platt, M. L. (2007). Monotonic coding of numerosity in macaque lateral intraparietal area. *PLoS Biology, 5*(8), e208.

Roitman, J. D., & Shadlen, M. N. (2002). Response of neurons in the lateral intraparietal area during a combined visual discrimination reaction time task. *Journal of Neuroscience, 22*(21), 9475–9489.

Rosa, M. G., & Tweedale, R. (2005). Brain maps, great and small: Lessons from comparative studies of primate visual cortical organization. *Philosophical Transactions of the Royal Society of London B: Biological Science, 360*(1456), 665–691.

Rousselet, G. A., Thorpe, S. J., & Fabre-Thorpe, M. (2004). How parallel is visual processing in the ventral pathway? *Trends in Cognitive Sciences, 8*(8), 363–370.

Roy, S., Jayakumar, J., Martin, P. R., Dreher, B., Saalmann, Y. B., Hu, D.,& Vidyasagar, T. R. (2009). Segregation of short-wavelength-sensitive (S) cone signals in the macaque dorsal lateral geniculate nucleus. *European Journal of Neuroscience, 30*(8), 1517–1526.

Rust, N. C., & Dicarlo, J. J. (2010). Selectivity and tolerance ("invariance") both increase as visual information propagates from cortical area V4 to IT. *Journal of Neuroscience, 30*(39), 12978–12995.

Salzman, C. D., Murasugi, C. M., Britten, K. H., & Newsome, W. T. (1992). Microstimulation in visual area MT: Effects on direction discrimination performance. *Journal of Neuroscience, 12*(6), 2331–2355.

Sasaki, Y., Rajimehr, R., Kim, B. W., Ekstrom, L. B., Vanduffel, W., & Tootell, R. B. (2006). The radial bias: A different slant on visual orientation sensitivity in human and nonhuman primates. *Neuron, 51*(5), 661–670.

Sato, T., Uchida, G., & Tanifuji, M. (2009). Cortical columnar organization is reconsidered in inferior temporal cortex. *Cerebral Cortex, 19*(8), 1870–1888.

Schluppeck, D., Glimcher, P., & Heeger, D. J. (2005). Topographic organization for delayed saccades in human posterior parietal cortex. *Journal of Neurophysiology, 94*(2), 1372–1384.

Schneider, K. A., Richter, M. C., & Kastner, S. (2004). Retinotopic organization and functional subdivisions of the human lateral geniculate nucleus: A high-resolution functional magnetic resonance imaging study. *Journal of Neuroscience, 24*(41), 8975–8985.

Schwartz, E. L., Desimone, R., Albright, T. D., & Gross, C. G. (1983). Shape recognition and inferior temporal neurons. *Proceedings of the National Academy of Sciences, USA, 80*(18), 5776–5778.

Schwarzlose, R. F., Swisher, J. D., Dang, S., & Kanwisher, N. (2008). The distribution of category and location information across object-selective regions in human visual cortex. *Proceedings of the National Academy of Sciences, USA, 105*(11), 4447–4452.

Sereno, A. B., & Maunsell, J. H. (1998). Shape selectivity in primate lateral intraparietal cortex. *Nature, 395*(6701), 500–503.

Sereno, M. I., Dale, A. M., Reppas, J. B., Kwong, K. K., Belliveau, J. W., Brady, T. J., . . . Tootell, R. B. (1995). Borders of multiple visual areas in humans revealed by functional magnetic resonance imaging. *Science, 268*(5212), 889–893.

Sereno, M. I., & Huang, R. S. (2006). A human parietal face area contains aligned head-centered visual and tactile maps. *Nature Neuroscience, 9*(10), 1337–1343.

Sereno, M. I., Pitzalis, S., & Martinez, A. (2001). Mapping of contralateral space in retinotopic coordinates by a parietal cortical area in humans. *Science, 294*(5545), 1350–1354.

Shadlen, M. N., & Newsome, W. T. (2001). Neural basis of a perceptual decision in the parietal cortex (area LIP) of the rhesus monkey. *Journal of Neurophysiology, 86*(4), 1916–1936.

Shapley, R., Hawken, M., & Xing, D. (2007). The dynamics of visual responses in the primary visual cortex. *Progress in Brain Research, 165,* 21–32.

Shapley, R., Kaplan, E., & Soodak, R. (1981). Spatial summation and contrast sensitivity of X and Y cells in the lateral geniculate nucleus of the macaque. *Nature, 292*(5823), 543–545.

Sheinberg, D. L., & Logothetis, N. K. (2001). Noticing familiar objects in real world scenes: The role of temporal cortical neurons in natural vision. *Journal of Neuroscience, 21*(4), 1340–1350.

Sherman, S. M., & Guillery, R. W. (2002). The role of the thalamus in the flow of information to the cortex. *Philosophical Transactions of the Royal Society of London B: Biological Science, 357*(1428), 1695–1708.

Shipp, S. (2007). Structure and function of the cerebral cortex. *Current Biology, 17*(12), R443–449.

Shipp, S., & Zeki, S. (2002a). The functional organization of area V2, I: Specialization across stripes and layers. *Visual Neuroscience, 19*(2), 187–210.

Shipp, S., & Zeki, S. (2002b). The functional organization of area V2, II: The impact of stripes on visual topography. *Visual Neuroscience, 19*(2), 211–231.

Shmuel, A., Korman, M., Sterkin, A., Harel, M., Ullman, S., Malach, R.,& Grinvald, A. (2005). Retinotopic axis specificity and selective clustering of feedback projections from V2 to V1 in the owl monkey. *Journal of Neuroscience, 25*(8), 2117–2131.

Shomstein, S., & Behrmann, M. (2006). Cortical systems mediating visual attention to both objects and spatial locations. *Proceedings of the National Academy of Sciences, USA, 103*(30), 11387–11392.

Silver, M. A., Ress, D., & Heeger, D. J. (2005). Topographic maps of visual spatial attention in human parietal cortex. *Journal of Neurophysiology, 94*(2), 1358–1371.

Sincich, L. C., Adams, D. L., & Horton, J. C. (2003). Complete flatmounting of the macaque cerebral cortex. *Visual Neuroscience, 20*(6), 663–686.

Sincich, L. C., & Horton, J. C. (2002a). Divided by cytochrome oxidase: A map of the projections from V1 to V2 in macaques. *Science, 295*(5560), 1734–1737.

Sincich, L. C., & Horton, J. C. (2002b). Pale cytochrome oxidase stripes in V2 receive the richest projection from macaque striate cortex. *Journal of Comparative Neurology, 447*(1), 18–33.

Sincich, L. C., & Horton, J. C. (2003). Independent projection streams from macaque striate cortex to the second visual area and middle temporal area. *Journal of Neuroscience, 23*(13), 5684–5692.

Sincich, L. C., & Horton, J. C. (2005a). The circuitry of V1 and V2: integration of color, form, and motion. *Annual Review of Neuroscience, 28,* 303–326.

Sincich, L. C., & Horton, J. C. (2005b). Input to V2 thin stripes arises from V1 cytochrome oxidase patches. *Journal of Neuroscience, 25*(44), 10087–10093.

Sincich, L. C., Jocson, C. M., & Horton, J. C. (2007). Neurons in V1 patch columns project to V2 thin stripes. *Cerebral Cortex, 17*(4), 935–941.

Sincich, L. C., Jocson, C. M., & Horton, J. C. (2010). V1 interpatch projections to v2 thick stripes and pale stripes. *Journal of Neuroscience, 30*(20), 6963–6974.

Sincich, L. C., Park, K. F., Wohlgemuth, M. J., & Horton, J. C. (2004). Bypassing V1: A direct geniculate input to area MT. *Nature Neuroscience, 7*(10), 1123–1128.

Smith, A. T., Singh, K. D., Williams, A. L., & Greenlee, M. W. (2001). Estimating receptive field size from fMRI data in human striate and extrastriate visual cortex. *Cerebral Cortex, 11*(12), 1182–1190.

Snyder, L. H., Grieve, K. L., Brotchie, P., & Andersen, R. A. (1998). Separate body- and world-referenced representations of visual space in parietal cortex. *Nature, 394*(6696), 887–891.

Solomon, S. G., & Lennie, P. (2007). The machinery of colour vision. *NatureReviews Neuroscience, 8*(4), 276–286.

Solomon, S. G., White, A. J., & Martin, P. R. (2002). Extraclassical receptive field properties of parvocellular, magnocellular, and koniocellular cells in the primate lateral geniculate nucleus. *Journal of Neuroscience, 22*(1), 338–349.

Stafford, D. K., & Dacey, D. M. (1997). Physiology of the A1 amacrine: A spiking, axon-bearing interneuron of the macaque monkey retina. *Visual Neuroscience, 14*(3), 507–522.

Stensaas, S. S., Eddington, D. K., & Dobelle, W. H. (1974). The topography and variability of the primary visual cortex in man. *Journal of Neurosurgery, 40*(6), 747–755.

Stepniewska, I., Qi, H. X., & Kaas, J. H. (1999). Do superior colliculus projection zones in the inferior pulvinar project to MT in primates? *European Journal of Neuroscience, 11*(2), 469–480.

Sterling, P. (2004). How retinal circuits optimize the transfer of visual information. In L. M. Chalupa & J. S. Werner (Eds.), *The visual neurosciences*. Cambridge, MA: MIT Press.

Stettler, D. D., Das, A., Bennett, J., & Gilbert, C. D. (2002). Lateral connectivity and contextual interactions in macaque primary visual cortex. *Neuron, 36*(4), 739–750.

Swisher, J. D., Halko, M. A., Merabet, L. B., McMains, S. A., & Somers, D. C. (2007). Visual topography of human intraparietal sulcus. *Journal of Neuroscience, 27*(20), 5326–5337.

Tanaka, K. (1996). Inferotemporal cortex and object vision. *Annual Review of Neuroscience, 19,* 109–139.

Tanaka, K., Saito, H., Fukada, Y., & Moriya, M. (1991). Coding visual images of objects in the inferotemporal cortex of the macaque monkey. *Journal of Neurophysiology, 66*(1), 170–189.

Tanigawa, H., Lu, H. D., & Roe, A. W. (2010). Functional organization for color and orientation in macaque V4. *Nature Neuroscience, 13*(12), 1542–1548.

Thomas, O. M., Cumming, B. G., & Parker, A. J. (2002). A specialization for relative disparity in V2. *Nature Neuroscience, 5*(5), 472–478.

Tootell, R. B., Silverman, M. S., De Valois, R. L., & Jacobs, G. H. (1983). Functional organization of the second cortical visual area in primates. *Science, 220*(4598), 737–739.

Tootell, R. B., Silverman, M. S., Hamilton, S. L., De Valois, R. L., & Switkes, E. (1988). Functional anatomy of macaque striate cortex. III. Color. *Journal of Neuroscience, 8*(5), 1569–1593.

Tootell, R. B., Silverman, M. S., Switkes, E., & De Valois, R. L. (1982). Deoxyglucose analysis of retinotopic organization in primate striate cortex. *Science, 218*(4575), 902–904.

Toth, L. J., & Assad, J. A. (2002). Dynamic coding of behaviourally relevant stimuli in parietal cortex. *Nature, 415*(6868), 165–168.

Tsao, D. Y., Freiwald, W. A., Knutsen, T. A., Mandeville, J. B., & Tootell, R. B. (2003). Faces and objects in macaque cerebral cortex. *Nature Neuroscience, 6*(9), 989–995.

Tsao, D. Y., Freiwald, W. A., Tootell, R. B., & Livingstone, M. S. (2006). A cortical region consisting entirely of face-selective cells. *Science, 311*(5761), 670–674.

Tsunoda, K., Yamane, Y., Nishizaki, M., & Tanifuji, M. (2001). Complex objects are represented in macaque inferotemporal cortex by the combination of feature columns. *Nature Neuroscience, 4*(8), 832–838.

Uka, T., & DeAngelis, G. C. (2003). Contribution of middle temporal area to coarse depth discrimination: Comparison of neuronal and psychophysical sensitivity. *Journal of Neuroscience, 23*(8), 3515–3530.

Uka, T., & DeAngelis, G. C. (2004). Contribution of area MT to stereoscopic depth perception: Choice-related response modulations reflect task strategy. *Neuron, 42*(2), 297–310.

Ullman, S. (1997). *High-level vision: Object recognition and visual cognition*. Cambridge, MA: MIT Press.

Umeda, K., Tanabe, S., & Fujita, I. (2007). Representation of stereoscopic depth based on relative disparity in macaque area V4. *Journal of Neurophysiology, 98*(1), 241–252.

Ungerleider, L. G., & Mishkin, M. (1982). Two cortical visual systems. In D. J. Ingle, R. J. W. Mansfield & M. S. Goodale (Eds.), *The analysis of visual behavior* (pp. 549–586). Cambridge, MA: MIT Press.

Van Essen, D. C. (2004). Organization of visual areas in macaque and human cerebral cortex. In L. M. Chalupa & J. S. Werner (Eds.), *The visual neurosciences* (Vol. 1, pp. 507–521). Cambridge, MA: MIT Press.

Van Essen, D. C., & Drury, H. A. (1997). Structural and functional analyses of human cerebral cortex using a surface-based atlas. *Journal of Neuroscience, 17*(18), 7079–7102.

Van Essen, D. C., Maunsell, J. H., & Bixby, J. L. (1981). The middle temporal visual area in the macaque: Myeloarchitecture, connections, functional properties, and topographic organization. *Journal of Comparative Neurology, 199*(3), 293–326.

Verweij, J., Hornstein, E. P., & Schnapf, J. L. (2003). Surround antagonism in macaque cone photoreceptors. *Journal of Neuroscience, 23*(32), 10249–10257.

von der Heydt, R., & Peterhans, E. (1989). Mechanisms of contour perception in monkey visual cortex. I. Lines of pattern discontinuity. *Journal of Neuroscience, 9*(5), 1731–1748.

von der Heydt, R., Peterhans, E., & Baumgartner, G. (1984). Illusory contours and cortical neuron responses. *Science, 224*(4654), 1260–1262.

Wandell, B. A., Dumoulin, S. O., & Brewer, A. A. (2007). Visual field maps in human cortex. *Neuron, 56*(2), 366–383.

Wassle, H. (2004). Parallel processing in the mammalian retina. *Nature Review Neuroscience, 5*(10), 747–757.

Wassle, H., & Boycott, B. B. (1991). Functional architecture of the mammalian retina. *Physiology Review, 71*(2), 447–480.

Wassle, H., Dacey, D. M., Haun, T., Haverkamp, S., Grunert, U., & Boycott, B. B. (2000). The mosaic of horizontal cells in the macaque monkey retina: With a comment on biplexiform ganglion cells. *Visual Neuroscience, 17*(4), 591–608.

Westheimer, G. (1979). Cooperative neural processes involved in stereoscopic acuity. *Experimental Brain Research, 36*(3), 585–597.

White, A. J., Solomon, S. G., & Martin, P. R. (2001). Spatial properties of koniocellular cells in the lateral geniculate nucleus of the marmoset *Callithrix jacchus*. *Journal of Physiology, 533*(Pt 2), 519–535.

Willmore, B. D., Prenger, R. J., & Gallant, J. L. (2010). Neural representation of natural images in visual area V2. *Journal of Neuroscience, 30*(6), 2102–2114.

Wilson, J. R., & Forestner, D. M. (1995). Synaptic inputs to single neurons in the lateral geniculate nuclei of normal and monocularly deprived squirrel monkeys. *Journal of Comparative Neurology, 362*(4), 468–488.

Winawer, J., Horiguchi, H., Sayres, R. A., Amano, K., & Wandell, B. A. (2010). Mapping hV4 and ventral occipital cortex: The venous eclipse. *Journal of Vision, 10*(5), 1.

Wunderlich, K., Schneider, K. A., & Kastner, S. (2005). Neural correlates of binocular rivalry in the human lateral geniculate nucleus. *Nature Neuroscience, 8*(11), 1595–1602.

Wurtz, R. H., Joiner, W. M., & Berman, R. A. (2011). Neuronal mechanisms for visual stability: Progress and problems. *Philosophical Transactions of the Royal Society of London B: Biological Science, 366*(1564), 492–503.

Xiao, Y., Wang, Y., & Felleman, D. J. (2003). A spatially organized representation of colour in macaque cortical area V2. *Nature, 421*(6922), 535–539.

Xu, X., Bonds, A. B., & Casagrande, V. A. (2002). Modeling receptive-field structure of koniocellular, magnocellular, and parvocellular LGN cells in the owl monkey (*Aotus trivigatus*). *Visual Neuroscience, 19*(6), 703–711.

Xu, X., Ichida, J. M., Allison, J. D., Boyd, J. D., Bonds, A. B., & Casagrande, V. A. (2001). A comparison of koniocellular, magnocellular, and parvocellular receptive field properties in the lateral geniculate nucleus of the owl monkey (*Aotus trivirgatus*). *Journal of Physiology, 531*(Pt 1), 203–218.

Yabuta, N. H., & Callaway, E. M. (1998). Functional streams and local connections of layer 4C neurons in primary visual cortex of the macaque monkey. *Journal of Neuroscience, 18*(22), 9489–9499.

Yabuta, N. H., Sawatari, A., & Callaway, E. M. (2001). Two functional channels from primary visual cortex to dorsal visual cortical areas. *Science, 292*(5515), 297–300.

Yacoub, E., Shmuel, A., Logothetis, N., & Ugurbil, K. (2007). Robust detection of ocular dominance columns in humans using Hahn Spin Echo BOLD functional MRI at 7 Tesla. *Neuroimage, 37*(4), 1161–1177.

Yamane, Y., Carlson, E. T., Bowman, K. C., Wang, Z., & Connor, C. E. (2008). A neural code for three-dimensional object shape in macaque inferotemporal cortex. *Nature Neuroscience, 11*(11), 1352–1360.

Yoshioka, T., Blasdel, G. G., Levitt, J. B., & Lund, J. S. (1996). Relation between patterns of intrinsic lateral connectivity, ocular dominance, and cytochrome oxidase-reactive regions in macaque monkey striate cortex. *Cerebral Cortex, 6*(2), 297–310.

Zeki, S. (1983). The distribution of wavelength and orientation selective cells in different areas of monkey visual cortex. *Philosophical Transactions of the Royal Society of London B: Biological Science, 217*(1209), 449–470.

Zeki, S. (2004). Thirty years of a very special visual area, Area V5. *Journal of Physiology, 557*(Pt 1), 1–2.

Zeki, S. M. (1973). Colour coding in rhesus monkey prestriate cortex. *Brain Research, 53*(2), 422–427.

Zeki, S. M. (1974). Functional organization of a visual area in the posterior bank of the superior temporal sulcus of the rhesus monkey. *Journal of Physiology, 236*(3), 549–573.

Zeki, S. M. (1978). Functional specialisation in the visual cortex of the rhesus monkey. *Nature, 274*(5670), 423–428.

Zhou, H., Friedman, H. S., & von der Heydt, R. (2000). Coding of border ownership in monkey visual cortex. *Journal of Neuroscience, 20*(17), 6594–6611.